ELSEVIER

International Journal of Solids and Structures 41 (2004) 4599–4634

INTERNATIONAL JOURNAL OF SOLIDS and STRUCTURES

www.elsevier.com/locate/ijsolstr

Rheological–dynamical analogy: visco-elasto-plastic behavior of metallic bars

Dragan D. Milašinović *

Department of Civil Engineering, University of Novi Sad, Subotica Kozaračka 2a, 24000 Subotica, Serbia and Montenegro

Received 7 August 2003; received in revised form 26 February 2004
Available online 15 April 2004

Abstract

This paper presents an application of the rheological–dynamical analogy (RDA) for describing the various aspects of a visco-elasto-plastic behavior of metallic bars related to standard tensile tests. The analogy has been developed on the basis of mathematical–physical analogy between a visco-elasto-plastic rheological model and a dynamical model with viscous damping, and is aimed to be used for the analysis of inelastic deforming of materials and structures. In this presentation, the aim will be to highlight the thermodynamics aspect of proportional stress through hysteretic loop dissipation, oscillation in the stress–strain curve (lower and upper yield point), transition from plasticity range, transition from strain hardening range, and RDA fracture stress of thin long metallic bars. This paper provides description of process of visco-elasto-plastic yielding and numerical example of obtaining isochronous σ–ε diagram of metallic bars using RDA similitude. In order to demonstrate the ability of the RDA modeling technique, the comparison with experimental and numerical results by [ASCE, J. Eng. Mech. 125(12) (1999) 1243] is presented. The presented RDA analysis can be readily used to perform precise shape of isochronous σ–ε diagrams of metallic bars. The RDA isochronous stress–strain diagram is used to predict the loading functions for the material of metallic bars.

Keywords: Rheological–dynamical analogy; RDA modulus; RDA similitude; Isochronous RDA σ–ε diagrams; Loading function

1. Introduction

About a century has passed since the widespread interest in the subject of inelastic behavior of load-carrying members began to develop. The subject has been divided broadly into two rather distinct areas. One area concerns the study of the inelastic behavior of members that are subjected to loads under environmental conditions (especially temperature and rate of loading) such that time is not a factor; this type of inelastic behavior is said to be time independent. For example, members made of most metals and subjected to static loads at room temperatures will exhibit time-independent inelastic behavior when the loads are increased beyond the elastic-limit load. The second area concerns the study of the inelastic behavior of

* Tel.: +381-24-554-300; fax: +381-24-554-580.
E-mail address: ddmil@gf.su.ac.yu (D.D. Milašinović).

0020-7683/$ - see front matter © 2004 Elsevier Ltd. All rights reserved.
doi:10.1016/j.ijsolstr.2004.02.061

members that are subjected to loads under environmental conditions such that time is a factor; this type of inelastic behavior is said to be time dependent. For example, members made of most plastic materials and subjected to static loads at room temperature will exhibit inelastic behavior, called creep, for all levels of the load. The longer the time of application of the static load, the greater is the magnitude of the inelastic deformation when creep occurs.

Although the overall behavior of mild steel members is well documented from many tests, the practical influence of strain hardening on load capacity, discontinuous plastic deformation, and creep effect has received little attention so far. The classical theory of plasticity is based on the assumption that the material is perfectly plastic with identical properties in tension and compression. The material does not exhibit strain hardening but flows plastically under constant stress. All limit design theories and most metal forming theories are based on these stress–strain relations. However, the phenomenon of discontinuous plastic deformation, which is more, pronounced in low than in high-purity metals (Bell, 1973, Section 4.31) cannot be obtained by above assumptions. If the tension test of a so-called ductile metal is made at higher rates of application of the load (that is, higher strain rates) than it is used in the ordinary standard procedure, the magnitude of the inelastic strain which precedes fracture may be greatly reduced and the stresses corresponding to any given strain may be raised (Elam, 1938). Conversely, the yield stress of the material may be lowered slightly if the strain rate is appreciably lower than one used in the ordinary standard procedure. In the tension test of a metal it will be recognized that, when low temperature is combined with high strain rates, the reduction that occurs in the magnitude of the inelastic strain preceding fracture is greater than when only one of these effects is present.

The phenomenon of discontinuous plastic deformation has been seriously considered from the beginning of the 19th Century up to today (Froli and Royer-Carfagni, 2000). The subject has been analyzed into two distinct ways. In one way of thinking, the oscillations can be attributed to the influence of the testing machine stiffness. Based on this concept Siebel and Schwaigerer (1937–1938) analyzed the influence of testing-device stiffness on the shape of the σ–ε diagrams. These results were later confirmed by Miklowitz (1947). The other approach considers them as the reflection of an internal material instability, irrespective of the loading device (Lempriere, 1962). The concept of distinction between an 'averaged' and a 'local' material response was suggested by Froli and Royer-Carfagni (1997, 1999, 2000).

The present paper represents an attempt to interpret the problems associated with the tensile response of metallic bars, both time independent and time dependent, in the unified manner by solving both types of problems using the same iterative rheological–dynamical analogy (RDA) procedure. After several years of research, the author has found that using the rheological–dynamical modulus relationship can solve both types of problems of isochronous stress–strain relationships. The fundamental statement of this theoretical tool and the governing differential equations have already been explained by Milašinović (2000) where RDA was used to predict the buckling behavior of slender columns. In the second paper, the author (Milašinović, 2003) demonstrates that RDA is also capable to model the fatigue behavior of axially, cyclically loaded bars.

In this paper the proportional stress or reaction-stress of clamped metal bar under axially fatigue process is obtained using physical characteristics of metal only, like as: specific heat, coefficient of linear thermal expansion and mass density. Elasticity stress of the bar under compression is obtained by RDA formula from which we have that elasticity stress also becomes dependent upon the dimensions of the bar (its length and diameter) and thus is no more a physical characteristics of the material only. In ductile materials like metals, some difference between point of proportionality and point of elasticity produce the deviation from perfect elasticity with dissipation of mechanical energy through quasi-viscous flow or visco-elastic creep. This is the reason of the drop in the stress–strain curve in the average σ–ε diagrams (upper-yield and lower-yield point). Transition from plasticity range continues until the magnitude of the error of the stress level for plastic yielding becomes lesser than some previously assigned value.

Strain hardening is the term used to define the increase in strength with increasing strain as plastic deformation or flow occurs beyond the lower-yield point. Strain hardening range is difficult to obtain by the experimental investigations, except determination the ultimate or fracture stress and strain. In the present paper this phenomena is explained in terms of visco-plastic yielding. Iterative RDA procedure for stress levels and strains for visco-plastic yielding, which include explanation of fatigue process and reduction of cross-section area with fracture of the bar, is derived. Bernoulli's energy theorem is used for the evaluation of the localized reduction of cross-section area. Transition from visco-plasticity range continues until the magnitude of the error of the stress level for visco-plastic yielding becomes lesser than some previously assigned value.

Loading functions for the material of metallic bars are obtained using by Hencky's total-strain theory under the assumption of compressibility in the plastic and assumption of incompressibility in the strain hardening range.

2. Rheological–dynamical analogy (RDA)

All inelastic deformation is time sensitive, and because of that the rheological analysis proves unavoidable. Elasticity, plasticity, viscosity and strength are essential rheological properties from which most of other complex properties may be derived (Reiner, 1955).

Creep properties are usually obtained from tension and compression specimens subjected to constant loads at constant temperature. A typical tension creep curve is shown in Fig. 1. The strain at zero time has an elastic component. A mechanical disturbance (strain) propagates in an elastic medium at the finite velocity $\sqrt{E_H/\rho}$. In a primary creep range, the creep rate continues to decrease with time. If the material exhibits a minimum strain rate σ_0/λ_K, the secondary creep rate designates the range of steady-state creep. At the end of the secondary creep range, the effect of the increase of stress is the speared because the reduction in cross-sectional area begins to influence on deformation so that the strain rate increases with

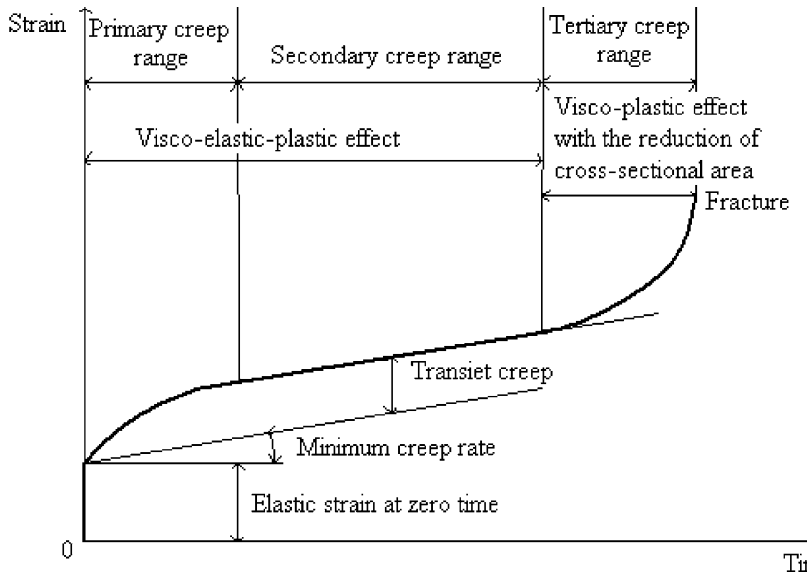

Fig. 1. Typical constant load–tension creep curve.

time until fracture occurs. The latter range of the creep curve may not exist for other states of stress; consequently the tertiary creep range is usually not considered in creep theories.

Every strain, in principle, is a function of time because a stress is always introduced into the body during a definite time interval (even a very small one) and therefore the isochronous stress–strain relationship must be included in the analysis of material effects. The significant aspect of the three phenomena of isochronous stress–strain relationships mentioned so far according to the RDA can be represented as indicated in Fig. 2. Path *APE* includes the elastic effect; path EY_LY_UC includes visco-elastic–plastic effect; path CD includes visco-plastic effect with reduction of cross-section area.

As stated earlier (path *APE*), the majority of materials are in the elastic and visco-elastic range in the conditions of low loading, whereas after reaching the yield stress, it transits to the visco-elastic–plastic (path EY_LY_UC) and visco-plastic (path *CD*) range.

Polakowski and Ripling (1966) has explained the flow, which occurs beyond the lower-yield point in terms of dislocation theory. Here, it is assumed that the strain is measured when the specified stress has been reached. Strain ε_E obtained in this way shall be considered to be independent of time, i.e. instantaneous. Elastic material behavior can be modeled by a linear spring (**H**). Therefore, instantaneous or initial strain should be $\varepsilon_E = \sigma_0/E_H$ where E_H is the elastic modulus. The time-dependent, or delayed, ε_{ve} and ε_{vp} strains are measured from the time, when the instantaneous strain has developed. Delayed elastic or visco-elastic strain ε_{ve} may be imagined as a common behavior of elastic E_K and viscous λ_K materials and modeled by Kelvin's model (**K**). The concept of delayed plastic or visco-plastic material behavior ε_{vp} may be imagined as a common behavior of the friction slider component σ_{SV} and viscous component λ_N of materials. The friction slider develops a stress σ_{SV}, becoming active only if $\sigma \geqslant Y = \sigma_Y + H' \cdot \varepsilon_{vp}(t)$, where σ is the total applied stress and Y is some limiting yield value. The stress level in the friction slider depends on whether the threshold or yield stress Y, has been reached. If the stress σ is discontinued, the friction slider does not return into its original position. Visco-plastic material behavior can be modeled by the third of the sequentially linked models (**N/StV**) as shown in Fig. 3. Initial strain rate should be $\dot{\varepsilon} = \sigma/\lambda_K + (\sigma - \sigma_Y)/\lambda_N$.

In general each isochronous stress–strain diagram can be accurately approximated by following structural (rheological) equation if strain can be represented as indicated in Fig. 1

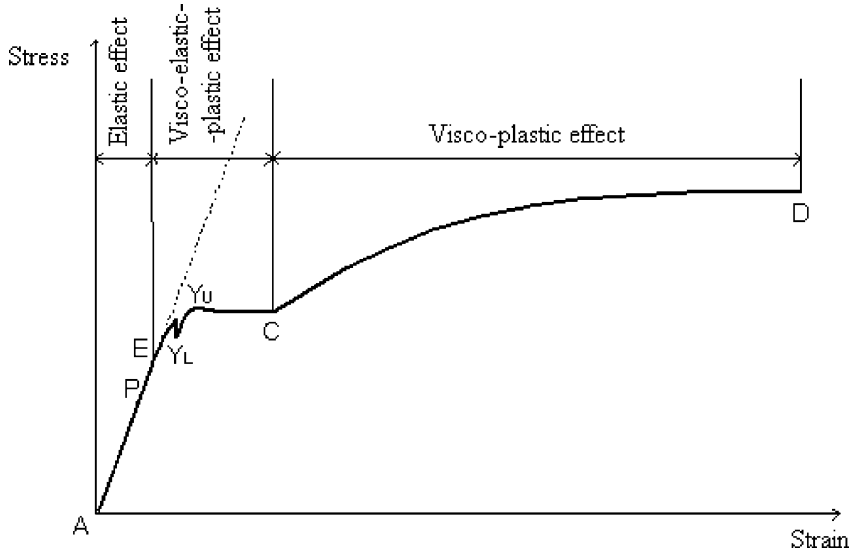

Fig. 2. Isochronous stress–strain curve illustrating elastic, visco-elastic–plastic and visco-plastic effects.

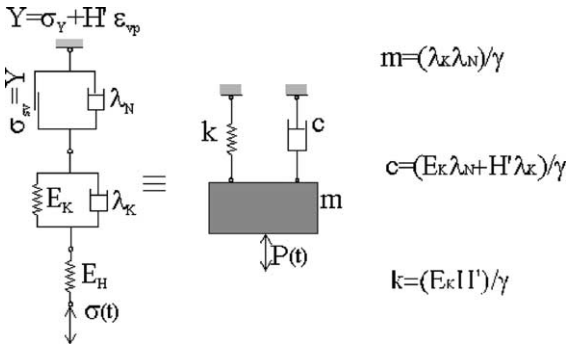

Fig. 3. Rheological–dynamical analogy.

$$\mathbf{H}-\mathbf{K}-(\mathbf{N}\,|\,\mathbf{StV}). \tag{1}$$

The governing differential equation has already been explained by (Milašinović, 2000)

$$\ddot{\varepsilon}(t)+\dot{\varepsilon}(t)\left(\frac{E_{\mathrm{K}}}{\lambda_{\mathrm{K}}}+\frac{H'}{\lambda_{\mathrm{N}}}\right)+\varepsilon(t)\frac{E_{\mathrm{K}}H'}{\lambda_{\mathrm{K}}\lambda_{\mathrm{N}}} =\frac{\ddot{\sigma}(t)}{E_{\mathrm{H}}}+\dot{\sigma}(t)\left(\frac{E_{\mathrm{K}}}{\lambda_{\mathrm{K}}E_{\mathrm{H}}}+\frac{H'}{\lambda_{\mathrm{N}}E_{\mathrm{H}}}+\frac{1}{\lambda_{\mathrm{K}}}+\frac{1}{\lambda_{\mathrm{N}}}\right)+\sigma(t)\left(\frac{E_{\mathrm{K}}}{\lambda_{\mathrm{K}}\lambda_{\mathrm{N}}}+\frac{H'}{\lambda_{\mathrm{K}}\lambda_{\mathrm{N}}}+\frac{E_{\mathrm{K}}H'}{\lambda_{\mathrm{K}}\lambda_{\mathrm{N}}E_{\mathrm{H}}}\right)-\sigma_{\mathrm{Y}}\frac{E_{\mathrm{K}}}{\lambda_{\mathrm{K}}\lambda_{\mathrm{N}}}. \tag{2}$$

The homogeneous equation of the inhomogeneous equation (2) has the following form:

$$\ddot{\varepsilon}(t)\lambda_{\mathrm{K}}\lambda_{\mathrm{N}}+\dot{\varepsilon}(t)(E_{\mathrm{K}}\lambda_{\mathrm{N}}+H'\lambda_{\mathrm{K}})+\varepsilon(t)E_{\mathrm{K}}H'=0, \tag{3}$$

where λ_{K}, λ_{N}, E_{K} and H' are given constants at fixed step time. Physical mechanism of the rheological–dynamical analogy and the governing equations between parameters where confirmed by Milašinović (2003).

Based on the analogy, one very complicate nonlinear visco-elasto-plastic problem may be solved as a simpler linear dynamical one.

Replacing $\lambda_{\mathrm{K}}\cdot\lambda_{\mathrm{N}}$ by $m\cdot\gamma$, $E_{\mathrm{K}}\cdot\lambda_{\mathrm{N}}+H'\cdot\lambda_{\mathrm{K}}$ by $c\cdot\gamma$ and $E_{\mathrm{K}}\cdot H'$ by $k\cdot\gamma$, the differential equation (3) becomes

$$\ddot{\varepsilon}(t)m+\dot{\varepsilon}(t)c+\varepsilon(t)k=0, \tag{4}$$

where

$$m=\frac{\lambda_{\mathrm{K}}\lambda_{\mathrm{N}}}{\gamma},\quad c=\frac{\left(E_{\mathrm{K}}\lambda_{\mathrm{N}}+H'\lambda_{\mathrm{K}}\right)}{\gamma},\quad k=\frac{E_{\mathrm{K}}H'}{\gamma}. \tag{5}$$

According to a dynamical model and the RDA the periodic stress may be expressed by means of the exponential function

$$\sigma''=\sigma_{\mathrm{A}}\mathrm{e}^{\mathrm{i}\omega_{\sigma}t}, \tag{6}$$

The strain lagging behind the stress by the phase difference α is given by

$$\varepsilon''=\varepsilon_{\mathrm{A}}\mathrm{e}^{\mathrm{i}(\omega_{\sigma}t-\alpha)}. \tag{7}$$

The complex modulus may be expressed by the ratio of the variable stress to the variable strain as follows:

$$E^{*}=\frac{\sigma''}{\varepsilon''}=\frac{\sigma_{\mathrm{A}}}{\varepsilon_{\mathrm{A}}}\mathrm{e}^{\mathrm{i}\alpha}. \tag{8}$$

According to the Moivre theorem, we have

$$e^{i\alpha} = \cos\alpha + i\sin\alpha. \tag{9}$$

Thus

$$E^* = \frac{\sigma_A}{\varepsilon_A}(\cos\alpha + i\sin\alpha), \tag{10}$$

where the dynamic and the loss modulus are

$$E_R = ReE^* = \frac{\sigma_A}{\varepsilon_A}\cos\alpha, \quad E_I = ImE^* = \frac{\sigma_A}{\varepsilon_A}\sin\alpha. \tag{11}$$

Among the various types of steady variable stresses, cyclic stresses are the most important; besides, these stresses are the most widely investigated. In addition, cyclic strain response does not depend much on the shape of the time curve within the cycle.

The curve in Fig. 4, which describes the variation of stresses in time, may considerably differ in appearance; variation of stresses in machine parts often follows the sinusoidal law

$$\sigma(t) = \sigma_0 + \sigma_A \sin(\omega_\sigma t), \tag{12}$$

where ω_σ is load or stress frequency. The maximum absolute stress in the cycle is denoted by σ_{max}, while the minimum is denoted by σ_{min}. The ratio of minimum stress to maximum with the signs taken into account is known as the cycle characteristic, or the coefficient of asymmetry of cycle

$$r = \frac{\sigma_{min}}{\sigma_{max}}. \tag{13}$$

The coefficient varies between −1 and +1. The half of the sum of maximum and minimum stresses of a cycle (taking into consideration their signs) is known as the constant component of cycle, or mean cycle stress

$$\sigma_0 = \frac{\sigma_{max} + \sigma_{min}}{2} = \frac{1+r}{2}\sigma_{max}. \tag{14}$$

The half of the difference of maximum and minimum stresses (also taking into consideration their signs) is known as the variable component of cycle or the amplitude of stresses in the cycle

$$\sigma_A = \frac{\sigma_{max} - \sigma_{min}}{2} = \frac{1-r}{2}\sigma_{max}. \tag{15}$$

The RDA equation due to sinusoidal stresses takes the form of

$$\ddot{\varepsilon}(t)m + \dot{\varepsilon}(t)c + \varepsilon(t)k = \sigma_A\left(\frac{k}{E_H} + \frac{E_K + H'}{\gamma} - \omega_\sigma^2\frac{m}{E_H}\right)\sin(\omega_\sigma t) + \sigma_A\left(\frac{c}{E_H} + \frac{\lambda_K + \lambda_N}{\gamma}\right)\omega_\sigma\cos(\omega_\sigma t) + \sigma_0\left(\frac{k}{E_H} + \frac{E_K + H'}{\gamma}\right) - \sigma_Y\frac{E_K}{\gamma}. \tag{16}$$

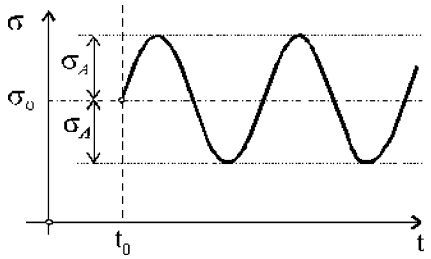

Fig. 4. Cyclic variation of stress.

The solution for this second-order differential equation with constant coefficients is

$$\varepsilon(t) = \varepsilon_{\mathrm{h}} + \varepsilon_{\mathrm{P}}, \tag{17}$$

where ε_{h} is the complementary solution and ε_{P} is the particular solution for the given equation

$$\varepsilon_{\mathrm{P}} = A\sin(\omega_\sigma t) + B\cos(\omega_\sigma t) + C, \tag{18}$$

where A, B and C are constants

$$A = \frac{P_\sigma(k - m\omega_\sigma^2) + Q_\sigma c\omega_\sigma}{(k - m\omega_\sigma^2)^2 + (c\omega_\sigma)^2}, \quad B = \frac{Q_\sigma(k - m\omega_\sigma^2) - P_\sigma c\omega_\sigma}{(k - m\omega_\sigma^2)^2 + (c\omega_\sigma)^2}, \quad C = \sigma_0\left(\frac{1}{E_{\mathrm{H}}} + \frac{1}{E_{\mathrm{K}}} + \frac{1}{H'}\right) - \sigma_{\mathrm{Y}}\frac{1}{H'}, \tag{19}$$

where

$$P_\sigma = \sigma_{\mathrm{A}}\left(\frac{k}{E_{\mathrm{H}}} + \frac{E_{\mathrm{K}} + H'}{\gamma}\right) - \sigma_{\mathrm{A}}\omega_\sigma^2\frac{m}{E_{\mathrm{H}}}, \quad Q_\sigma = \sigma_{\mathrm{A}}\left(\frac{c}{E_{\mathrm{H}}} + \frac{\lambda_{\mathrm{K}} + \lambda_{\mathrm{N}}}{\gamma}\right)\omega_\sigma. \tag{20}$$

Strain under constant stress, taking into consideration delayed elastic or visco-elastic strain is

$$\varepsilon'(t) = \varepsilon_h + C = \varepsilon^{\mathrm{c}} = \frac{\sigma_0}{E_{\mathrm{H}}} + \frac{\sigma_0}{E_{\mathrm{K}}}\left(1 - \mathrm{e}^{-(t/T_{\mathrm{K}})}\right) = \frac{\sigma_0}{E_{\mathrm{H}}(t_0)}(1 + \varphi). \tag{21}$$

where creep coefficient is

$$\varphi(t) = \frac{\varepsilon_{\mathrm{ve}}}{\varepsilon_{\mathrm{el}}} = \frac{E_{\mathrm{H}}(t_0)}{E_{\mathrm{K}}}\left(1 - \mathrm{e}^{-(t/T_{\mathrm{K}})}\right). \tag{22}$$

Cyclic strain is given by

$$\varepsilon_{\mathrm{p}}''(t) = A\sin(\omega_\sigma t) + B\cos(\omega_\sigma t) \tag{23}$$

or

$$\varepsilon_{\mathrm{p}}''(t) = \varepsilon_{\mathrm{A}}\sin(\omega_\sigma t - \alpha), \tag{24}$$

where cyclic strain amplitude and phase difference by which the strain lags behind the stress are

$$\varepsilon_{\mathrm{A}} = \sqrt{\frac{P_\sigma^2 + Q_\sigma^2}{(k - m\omega_\sigma^2)^2 + (c\omega_\sigma)^2}}, \tag{25}$$

$$\tan\alpha = \frac{P_\sigma c\omega_\sigma - Q_\sigma(k - m\omega_\sigma^2)}{P_\sigma(k - m\omega_\sigma^2) + Q_\sigma c\omega_\sigma}. \tag{26}$$

When the structural member is loaded cyclically, the rheological behavior of the member must be characterized by the dynamic time of retardation $T_{\mathrm{K}}^{\mathrm{D}}$. Now, taking into account formula (22) we have RDA visco-elastic modulus

$$E_{\mathrm{K}}^{\mathrm{D}}(t, t_0) = \frac{E_{\mathrm{H}}(t_0)}{\varphi(t)}\left(1 - \mathrm{e}^{-(t/T_{\mathrm{K}}^{\mathrm{D}})}\right) = \frac{E_{\mathrm{H}}(t_0)}{\varphi(t)}, \tag{27}$$

where

$$\mathrm{e}^{-(t/T_{\mathrm{K}}^{\mathrm{D}})} \approx 0. \tag{28}$$

Using Eqs. (25) and (26) we find rheological–dynamic (RDA) modulus as follows:

$$E_{\mathrm{R}} = \sigma_{\mathrm{A}} \frac{P_\sigma(k - m\omega_\sigma^2) + Q_\sigma c\omega_\sigma}{P_\sigma^2 + Q_\sigma^2}. \tag{29}$$

Substituting the dynamic time of retardation, $T_{\mathrm{K}}^{\mathrm{D}} = 1/\omega$ in Eq. (29) we obtain the RDA modulus which define the isochronous stress–strain relationship in the following form:

$$E_{\mathrm{R}}(t,t_0) = \frac{\frac{1+\delta^2}{E_{\mathrm{H}}(t_0)} + \frac{1}{E_{\mathrm{K}}^{\mathrm{D}}(t,t_0)} + \frac{1}{H'^{\mathrm{D}}(t,t_0)}}{\frac{1+\delta^2}{E_{\mathrm{H}}^2(t_0)} + \left(\frac{1}{E_{\mathrm{K}}^{\mathrm{D}}(t,t_0)} + \frac{1}{H'^{\mathrm{D}}(t,t_0)}\right)\left(\frac{2}{E_{\mathrm{H}}(t_0)} + \frac{1}{E_{\mathrm{K}}^{\mathrm{D}}(t,t_0)} + \frac{1}{H'^{\mathrm{D}}(t,t_0)}\right)}, \tag{30}$$

where

$$\delta = \frac{\omega_\sigma}{\omega} = \omega_\sigma T_{\mathrm{K}}^{\mathrm{D}}. \tag{31}$$

3. Proportional stress

3.1. Heat and work: determining the proportional stress

The study of the quantitative relationships between heat and other forms of energy is called thermodynamics. In this paper we shall be concerned with the relation of thermal expansion work to fictitious heat energy, taking the RDA into account.

For example, if we alternately subject an isolated steel bar (adiabatic process) to a large number of tensions and compressions under the stress $\sigma_{\max} = \sigma_{\mathrm{P}}$ (axial fatigue), we shall observe after a definite number of such changes in stress some viscous flow of steel, the strain lags the stress, and this is range when the fatigue appears.

When bar is stretched, the elastic potential energy is stored in the material (see Fig. 5). The work required to stretch or compress the bar does not depend on the weight of the bar. Consequently, gravity is not involved in the measurement of elastic potential energy U_1. Instead, the work required for the stretching or compressing depends upon the elasticity of the model

$$U_1 = \frac{\sigma_{\mathrm{P}}^2}{2E_{\mathrm{H}}} A l_0. \tag{32}$$

Consider a elliptical loop of the rheological–dynamical model shown in Fig. 5, where

$$\sigma''(t) = c\dot{\varepsilon}_{\mathrm{p}}''(t) = c\omega_\sigma \varepsilon_{\mathrm{A}} \cos(\omega_\sigma t - \alpha). \tag{33}$$

For a cyclic stress variation along the entire loop, the rate of release of visco-elastic energy is equal to the area enclosed by the loop, i.e.

$$W_{\mathrm{d,ve}} = \pi c\omega_\sigma \varepsilon_{\mathrm{A}}^2 \left[\frac{J}{M^2}\right]. \tag{34}$$

The cyclic strain amplitude ε_{A} have already been explained by Milašinović (2003), where RDA was used to predict the fatigue limit

$$\varepsilon_{\mathrm{A}} = \frac{\sigma_{\mathrm{A}}}{E_{\mathrm{H}}(t_0)} \sqrt{\frac{(1+\varphi^*)^2 + \delta^2}{1+\delta^2}}, \tag{35}$$

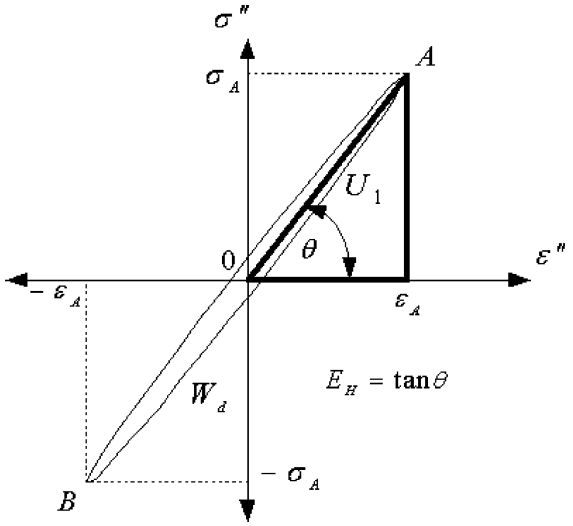

Fig. 5. Elastic potential energy and hysteretic loop dissipation in terms of stress–strain diagram.

where φ^* is structural creep coefficient. $T_{\mathrm{K}}^{\mathrm{D}} = 1/\omega$ and then the damping c (see Eq. (5)) is given by

$$c = 2kT_{\mathrm{K}}^{\mathrm{D}} = c_c. \tag{36}$$

Thus the rate of release of visco-elastic energy is given by

$$W_{\mathrm{d,ve}}(r) = \pi k \frac{1}{E_{\mathrm{H}}^2} \frac{(1-r)^2}{2} \sigma_{\mathrm{P}}^2 \frac{(1+\varphi^*)^2 + \delta^2}{1+\delta^2} \delta. \tag{37}$$

The area of transfer of energy is cross-sectional area A, and the energy dissipation is given by

$$U_{\mathrm{d}} = AW_{\mathrm{d,ve}}. \tag{38}$$

In the special case, at $\varphi^* \to 0$, we have elastic behavior and the rate of release of elastic energy from formula (37) as follows:

$$W_{\mathrm{d,E}}(r) = \pi k \frac{1}{E_{\mathrm{H}}^2} \frac{(1-r)^2}{2} \sigma_{\mathrm{P}}^2 \delta. \tag{39}$$

It can easily be shown that the total potential energy of the system $\Pi = U_1 - W$ decreases as a temperature of the system rise. When all elastic potential energy is converted through hysteretic loop dissipation, we have

$$U_{\mathrm{d}} = U_1 \tag{40}$$

and relative frequency $\delta_{\mathrm{e}}(r)$ for theoretical estimation of the fatigue life is

$$\frac{(1+\varphi^*)^2 + \delta_{\mathrm{e}}^2(r)}{1+\delta_{\mathrm{e}}^2(r)} \delta_{\mathrm{e}}(r) = U_1 \frac{2E_{\mathrm{H}}^2}{A\pi k(1-r)^2 \sigma_{\mathrm{P}}^2} = \frac{l_0 E_{\mathrm{H}}}{\pi k(1-r)^2}. \tag{41}$$

As mentioned above, high cycle frequencies during the cycling adiabatic process cause significant temperature rise in the isolated bar with both edges clamped, Fig. 6, and thermal expansion work W_{T}, as follows:

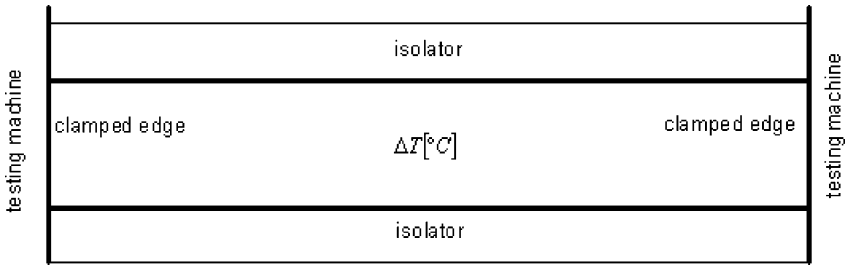

Fig. 6. Schematic representation of the bar in the fatigue test.

$$W_{\mathrm{T}} = \frac{E_{\mathrm{H}}(\alpha_{\mathrm{T}}\Delta T)^2}{2} A l_0. \tag{42}$$

α_{T} is a coefficient of linear thermal expansion, ΔT [°C] is the difference between the final temperature and the original temperature of the bar and E_{H} is Young's modulus.

However, when all elastic potential energy is converted through hysteretic loop dissipation we also have

$$U_{\mathrm{d}} = W_{\mathrm{T}}. \tag{43}$$

From Eq. (43) we may obtain difference between the final temperature and the original temperature of the bar as follows:

$$\Delta T_{\mathrm{ve}} = \frac{1}{\alpha_{\mathrm{T}}} \sqrt{\frac{1}{\delta_{\mathrm{e}}(r)} \frac{(1+\varphi^*)^2 + \delta^2}{1+\delta^2} \delta \frac{\sigma_{\mathrm{P}}}{E_{\mathrm{H}}}}. \tag{44}$$

In the special case at $\varphi^* \to 0$ (perfect elasticity), we have

$$\Delta T_{\mathrm{E}} = \frac{1}{\alpha_{\mathrm{T}}} \sqrt{\frac{\delta}{\delta_{\mathrm{e}}(r)} \frac{\sigma_{\mathrm{P}}}{E_{\mathrm{H}}}}, \tag{45}$$

where $\delta = \delta_1 N$ (N is the number of cycles) and σ_{P} is applied proportional stress. When it is fatigue reached, $\delta = \delta_{\mathrm{e}}(r)$ and thus

$$\Delta T_{\mathrm{E}} = \frac{1}{\alpha_{\mathrm{T}}} \frac{\sigma_{\mathrm{P}}}{E_{\mathrm{H}}}. \tag{46}$$

The amount of the fictitious heat in an isothermal process which must be added to the metal rod to simulate the observed temperature change is

$$Q = mc\Delta T_{\mathrm{E}} = \rho A l_0 c \Delta T_{\mathrm{E}}, \tag{47}$$

where c is specific heat of the metal. Hooke's law states that within the limits of perfect elasticity, strain is directly proportional to stress σ_{P}. Therefore we may state the first law of thermodynamics as follows: when all elastic potential energy in an adiabatic fatigue process is converted through hysteretic loop dissipation with temperature change to produce thermal expansion work, or when fictitious heat is added to the steel rod to simulate the observed temperature change, there is no loss of energy. Thus

$$W_{\mathrm{T}} = Q = \frac{E_{\mathrm{H}}\alpha_{\mathrm{T}}^2 \Delta T_{\mathrm{E}}^2}{2} A l_0 = \rho A l_0 c \Delta T_{\mathrm{E}} \Rightarrow \Delta T_{\mathrm{E}} = \frac{2\rho c}{E_{\mathrm{H}}\alpha_{\mathrm{T}}^2}. \tag{48}$$

Substituting ΔT_E in Eq. (46), we obtain the proportional stress as reaction-stress of clamped metal rod as follows:

$$\sigma_P = \frac{2\rho c}{\alpha_T}. \tag{49}$$

The proportional strain is $\varepsilon_P = \sigma_P / E_H$.

3.2. Steel bar as prototype

The fatigue behavior of axially loaded steel bars has already been explained by Milašinović (2003). The specimen on which, the work was done was an isolated reinforced steel bar: $l_0 = 50$ cm, $\phi = 1.9$ cm, $c = 0.113$ kcal/(kg C), $\alpha_T = 0.0000125$ 1/°C, $\rho = 7860$ kg/m^3, $E_H = 2.1 \times 10^5$ MPa. The bar is loaded with cyclic sinusoidal load in symmetrical cycle: $\sigma_0 = 0$, $\sigma_A = \sigma_P = 141$ MPa and frequency, $f = 20$ Hz.

Elastic potential energy

$$U_1 = \frac{\sigma_P^2}{2E_H} A l_0 = \frac{141^2}{2 \cdot 2.1 \times 10^5} \frac{0.019^2 \pi}{4} 0.5 = 6.71 \text{ J}.$$

When it is fatigue reached (see Milašinović, 2003, Table 2 and Fig. 12) we have $\delta_e(r) = 70.167$, $\Delta T_E = 53.71$ °C, and $W_{d,E} = 23667.78$ J/m^2. Thus
Energy dissipation

$$U_d = W_{d,E} A = 23667.78 \frac{0.019^2 \pi}{4} = 6.71 \text{ J}$$

Thermal expansion work

$$W_T = \frac{2.1 \times 10^{11} (0.0000125 \cdot 53.71)^2}{2} \frac{0.019^2 \pi}{4} 0.5 = 6.71 \text{ J}$$

Proportional stress as reaction-stress of clamped steel bar

$$\sigma_P = \frac{2\rho c}{\alpha_T} = \frac{2 \cdot 7860 \cdot 0.113}{0.0000125} = 142\,108\,800 \text{ Pa} = 142 \text{ MPa}$$

Reaction stress of clamped steel bar ($\sigma_P = 142$ MPa) is in excellent accordance with applied proportional stress ($\sigma_A = \sigma_P = 141$ MPa) from the axial fatigue experiment.

3.3. Metallic bars

Proportional stress of clamped steel bar in axial fatigue process (see Eq. (49)) is obtained using physical characteristics of the metal only, like as: specific heat of the metal c, coefficient of linear thermal expansion α_T and mass density ρ.

For the other metallic bars proportional stresses are shown in Table 1. The values of physical characteristics of metals: c, α_T, ρ and E_H are taken form the handbook of Modern Physics (Williams et al., 1968).

Table 1
Proportional stress of metallic bars

	Aluminum	Copper	Brass	Lead	Steel prototype
c [kcal/kg °C]	0.124	0.0924	0.0917	0.0305	0.113
ρ [kg/m^3]	2700	8930	8600	11310	7860
α_T [1/°C]	0.0000238	0.0000168	0.0000193	0.0000294	0.0000125
σ_p [N/m^2]	48 554 622	98 230 000	81 722 230	23 466 327	1.42E + 08
E_H [N/m^2]	69 600 000 000	1.16E + 11	90 200 000 000	15 700 000 000	2.1E + 11
ϵ_p	0.000698	0.000847	0.000906	0.001495	0.000677

4. Elasticity stress

4.1. Dimensional analysis and the RDA similitude

Dimensional analysis is the mathematics of dimensions of quantities and is another useful tool of rheological–dynamical analogy. In an equation expressing a physical relationship between quantities, absolute numerical and dimensional equality must exist.

The first equation of RDA (see Eq. (5)) is

$$m = \frac{\lambda_K \lambda_N}{\gamma},$$

where λ is Trouton viscosity. Trouton viscosity is the extensional viscosity, then the yields the following relation between shear viscosity η and extensional viscosity λ of Newtonian liquids:

$$\lambda = 3\eta. \tag{50}$$

The last equality is known as Trouton's formula. The product of the mass of a body and its velocity is called momentum; $m \cdot v$. Viscosity is transfer of momentum. Thus

$$\lambda = \frac{mv}{A}, \tag{51}$$

where A is the area of transfer of momentum.

4.2. Some important numbers using the RDA

Dividing the product of viscosity from Eq. (51) by the product of viscosity from the RDA we get

$$\frac{\left(\frac{mv}{A}\right)^2}{\lambda_K \lambda_N} = \frac{\left(\frac{\rho A l_0 v}{A}\right)^2}{\lambda_K \lambda_N} = \frac{\rho^2 l_0^2 v^2}{\lambda_K \lambda_N}. \tag{52}$$

The square root of this ratio

$$N_R^{RDA} = \frac{\rho l_0 v}{\sqrt{\lambda_K \lambda_N}}, \tag{53}$$

may be called the RDA Reynolds number. This number is known in fluid mechanics as

$$N_R = \frac{\rho v l_0}{\eta}. \tag{54}$$

Newton's second law of motion can be expressed in several different ways. For example, if we use the first RDA relationship, we get

$$m = \frac{\lambda_K \lambda_N}{\gamma} = \frac{\lambda_K \lambda_N}{\rho a} \Rightarrow ma = F = \frac{\lambda_K \lambda_N}{\rho}. \tag{55}$$

The stress is the ratio of the internal force F to the cross-section area A. Thus

$$\sigma = \frac{F}{A} = \frac{\lambda_K \lambda_N}{A\rho} = \frac{\rho^2 l_0^2 v^2}{A\rho} = \frac{\rho l_0^2 v^2}{A}. \tag{56}$$

Dividing the previous equation by stress σ we get RDA Euler number

$$N_E^{RDA} = \frac{\rho l_0^2 v^2}{\sigma A}. \tag{57}$$

This number is known in fluid mechanics as

$$N_E = \frac{\rho v^2}{p}, \tag{58}$$

where p is pressure. The elastic force F_E required to stretch a Hooke's spring is given by the formula

$$F_E = k\Delta l, \tag{59}$$

where k is the axial stiffness

$$k = \frac{E_H A}{l_0}. \tag{60}$$

Dividing the internal force F by the elastic force F_E we get RDA Cauchy number

$$N_C^{RDA} = \frac{\rho l_0^2 v^2}{\frac{E_H A}{l_0}\Delta l} = \frac{\rho v^2}{E_H}\frac{l_0^3}{A\Delta l}. \tag{61}$$

This number is known in fluid mechanics as

$$N_C = \frac{\rho v^2}{E_H}. \tag{62}$$

The square root of this number is known as the Mach number

$$N_M = \frac{v}{\sqrt{\frac{E_H}{\rho}}}. \tag{63}$$

Dividing the internal force F by the gravitational force $F = mg = \rho A l_0 g$ we get

$$\frac{\rho l_0^2 v^2}{\rho A l_0 g} = \frac{v^2}{g}\frac{l_0}{A}. \tag{64}$$

The square root of this ratio

$$N_F^{RDA} = v\sqrt{\frac{l_0}{gA}}, \tag{65}$$

may be called the RDA Froude number. This number is known in fluid mechanics as

$$N_F = \frac{v}{\sqrt{l_0 g}}. \tag{66}$$

In general, an engineer is concerned with the effect of the dominant force. In most rheological problem, gravity, viscosity, elasticity and plasticity govern predominantly, but not necessarily simultaneously.

4.3. Determining the elasticity stress of metallic bars

Crystalline materials like metals consist of a very large number of extremely small crystals. Each of these is a system of atoms arranged very close to each other in regular rows. These rows form the so-called crystalline lattice. The deformation of bodies takes place due to a change in the location of atoms, i.e. due to their getting closer or farther. Elastic deformation disappears when the force causing the deformation is removed; in this case, the body completely regains its initial shape and dimensions. This deformation occurs due to elastic distortion in the crystalline lattice. It has been experimentally observed that the elastic deformation continues till the forces being applied do not exceed a certain limit. Elasticity compressive stress of two-hinged bar is defined by Euler's formula

$$\sigma_{\mathrm{E}} = \frac{E_{\mathrm{H}}\pi^2}{\left(\frac{l_0}{k_z}\right)^2_{\mathrm{E}}}, \tag{67}$$

where $(l_0/k_z)_{\mathrm{E}} = \lambda^*_{\mathrm{E}}$ is slenderness ratio at the point of elasticity, E. In this way the elasticity stress also becomes dependent upon the dimensions of the bar (its length and diameter) and thus is no more a physical characteristics of the material only.

Euler's formula for critical force of bar under compression was obtained by integrating the differential equation of the deflected axis, i.e. it was derived on the assumption that the stresses in the bar are less than the limit of elasticity when it loses its stability. Consequently, we cannot use the critical stresses calculated by Euler's formula if they exceed the limit of elasticity of the given material. Generally, the stress–strain curve is linear elastic until $\sigma \leqslant \sigma_{\mathrm{E}}$ and nonlinear with considerable visco-elasto-plastic strain, under stress $\sigma \geqslant \sigma_{\mathrm{E}}$.

4.3.1. Steel bar as prototype

Axial fatigue experiment was performed on the isolated reinforced steel bar: $l_0 = 50$ cm, $\phi = 1.9$ cm, $E_{\mathrm{H}} = 2.1 \times 10^5$ MPa where

$$I_z = \frac{\phi^4\pi}{64}, \quad A = \frac{\phi^2\pi}{4}, \quad k_z = \sqrt{\frac{I_z}{A}} = \frac{\phi}{4} = \frac{1.9}{4} = 0.475, \left(\frac{l_0}{k_z}\right)_{\mathrm{E}} = \frac{4\cdot 50}{1.9} = 105.26,$$

$$\sigma_{\mathrm{E}} = \frac{210\,000\pi^2}{105.26^2} = 187 \text{ MPa}, \quad \varepsilon_{\mathrm{E}} = \frac{\sigma_{\mathrm{E}}}{E_{\mathrm{H}}} = \frac{187}{210\,000} = 0.000891.$$

As indicated in Milašinović (2000), is the fact that point of elasticity (E) of this steel is in good accordance with slenderness ratio of 105.26, because elastic Euler's theory for this type of low-carbon steel (Fe E275: $\sigma_{\mathrm{Y}} = 275$ N/mm^2; $\sigma_C = 390$ N/mm^2, according to prEN 10113) is not valid for slenderness ratio under the 104.

4.3.2. Metallic bars as true models

Rheological–dynamical models, in general may be either true models or distorted models. True models have all the significant characteristics of the prototype. Assuming the RDA similitude of metallic bars we can determine the elasticity stress (see Table 2), taking into account the RDA Euler number. Let us calculate the RDA Euler number using the velocity of the particles $v = \sigma/\sqrt{E_{\mathrm{H}}\rho}$,

$$N^{\mathrm{RDA}}_{\mathrm{E}} = \frac{\rho l_0^2 v^2}{\sigma A} = \frac{\rho l_0^2}{\sigma A}\frac{\sigma^2}{E_{\mathrm{H}}\rho} = \frac{l_0^2\sigma}{E_{\mathrm{H}}A}. \tag{68}$$

At the point of proportionality, P, RDA similitude of metallic bars with the same cross-section area, A is expressed by the formula

Table 2
Elasticity stress of metallic bars

	Aluminum	Copper	Brass	Lead	Steel prototype
ϵ_p	0.000698	0.000847	0.000906	0.001495	0.000677
E_H [N/m^2]	69 600 000 000	1.16E + 11	90 200 000 000	15 700 000 000	2.1E + 11
l_0 [cm]	49.24	44.70	43.22	33.647	50
l_0/k_2	103.67	94.11	90.99	70.84	105.26
σ_E [N/m^2]	63 917 966	1 29 270 577	1 07 520 933	30 881 553	187 000 000
ε_E	0.00091836	0.0011144	0.0011920	0.00196698	0.000891

$$N_E^{RDA} = \frac{l_0^2}{A}\frac{\sigma_P}{E_H} = \frac{l_0^2}{A}\varepsilon_P \Rightarrow \frac{l_{0,pr}^2}{A}\varepsilon_{P,pr} = \frac{l_{0,tm}^2}{A}\varepsilon_{P,tm} \Rightarrow l_{0,tm} = l_{0\,pr}\sqrt{\frac{\varepsilon_{P,pr}}{\varepsilon_{P,tm}}}. \tag{69}$$

4.4. Determining the structural (visco-elastic) creep coefficient of metallic bars

The deviation from perfect elasticity of the deformational response to applied force in continuous, homogeneous, isotropic solids may be attributed to dissipation of mechanical energy through quasi-viscous flow or creep of quasi-fluid components produces the visco-elastic response.

The creep coefficient is defined as the ratio of the visco-elastic strain of metallic bar to the elastic strain. Therefore, it may be determined using RDA similitude between Euler's and RDA elasticity stress.

Putting the Euler's elasticity stress into the expression of the RDA Euler number, we get

$$N_E^{RDA} = \frac{l_0^2}{A}\frac{\sigma_E}{E_H} = \frac{l_0^2}{\frac{\phi^2\pi}{4}}\frac{1}{E_H}\frac{E_H\pi^2}{\left(\frac{4l_0}{\phi}\right)^2} = \frac{\pi}{4}. \tag{70}$$

RDA expression of the elasticity stress is given by Milašinović (2000)

$$\sigma_E^{RDA} = \frac{E_H}{\frac{l_0}{k_z}\frac{k_z^3}{I_z}\frac{1}{\gamma\varphi^*}}, \tag{71}$$

where $k_z^3/I_z = 1/\phi\pi$. Now, we have RDA Euler number as follows:

$$N_E^{RDA} = \frac{l_0^2}{A}\frac{\sigma_E^{RDA}}{E_H} = \frac{l_0^2}{\frac{\phi^2\pi}{4}}\frac{1}{E_H}\frac{E_H\gamma\varphi^*}{\frac{4l_0}{\phi}\frac{1}{\phi\pi}} = l_0\gamma\varphi^*. \tag{72}$$

Comparing two expressions for the RDA Euler's numbers, we get the following structural creep coefficient:

$$\frac{\pi}{4} = l_0\gamma\varphi^* \Rightarrow \varphi^* = \frac{\pi}{4l_0\gamma}. \tag{73}$$

Table 3
Structural (visco-elastic) creep coefficient of metallic bars

	Aluminum	Copper	Brass	Lead	Steel prototype
γ [kg/cm^3]	2.70×10^{-3}	8.93×10^{-3}	8.60×10^{-3}	11.31×10^{-3}	7.86×10^{-3}
l_0 [cm]	49.24	44.70	43.22	33.647	50
φ^*	5.907559	1.9657373	2.113035	2.063863	1.998469
$\varepsilon_{\pi e}$	0.005425	0.002193	0.002519	0.004059	0.00178

The values of structural creep coefficient for the metallic bars are listed in Table 3. According to the definition of the creep coefficient we obtain visco-elastic strain as follows:

$$\varepsilon_{\mathrm{ve}} = \varphi^{*}\varepsilon_{\mathrm{E}}. \tag{74}$$

5. Visco-elastic–plastic range

5.1. The RDA modulus

If the external force exceeds the elasticity limit E, the body fails to regain completely its initial shape and size after the force is removed; the difference in size which thus remains is called the plastic (residual) deformation. In crystalline materials, this deformation is caused by the irreversible displacement of one layer of crystalline lattice with respect to the other. After the removal of external forces the displaced layers of atoms retain their position.

Real part of complex modulus (see Eq. (30)) is a measure of the energy dissipation of mechanical energy through visco-elasto-plastic flow

$$E_{\mathrm{R}}(t,t_0) = \frac{\frac{1+\delta^2}{E_{\mathrm{H}}(t_0)} + \frac{1}{E_{\mathrm{K}}^{\mathrm{D}}(t,t_0)} + \frac{1}{H'^{\mathrm{D}}(t,t_0)}}{\frac{1+\delta^2}{E_{\mathrm{H}}^2(t_0)} + \left(\frac{1}{E_{\mathrm{K}}^{\mathrm{D}}(t,t_0)} + \frac{1}{H'^{\mathrm{D}}(t,t_0)}\right)\left(\frac{2}{E_{\mathrm{H}}(t_0)} + \frac{1}{E_{\mathrm{K}}^{\mathrm{D}}(t,t_0)} + \frac{1}{H'^{\mathrm{D}}(t,t_0)}\right)}.$$

In the special case, when $\delta \to 0$, we have static loading and RDA modulus as follows:

$$E_{\mathrm{R}} = \frac{1}{\left(\frac{1}{E_{\mathrm{H}}} + \frac{1}{E_{\mathrm{K}}} + \frac{1}{H'}\right)}. \tag{75}$$

As started earlier, in the stage of low loading the majority of materials are in the range of visco-elasticity ($H' \to \infty$) with RDA modulus

$$E_{\mathrm{R}} = \frac{1}{\left(\frac{1}{E_{\mathrm{H}}} + \frac{1}{E_{\mathrm{K}}}\right)}, \tag{76}$$

where E_{K}, (see Eq. (27)) is

$$E_{\mathrm{K}} = \frac{E_{\mathrm{H}}}{\varphi^{*}}. \tag{77}$$

For a computed first value of E_{R} we can determine the appropriate first slope of the plastic strain

$$H'(\varepsilon_{\mathrm{p}}) = \frac{\mathrm{d}\sigma}{\mathrm{d}\varepsilon_{\mathrm{p}}} = \frac{\mathrm{d}\sigma}{\mathrm{d}\varepsilon - \mathrm{d}\varepsilon_{\mathrm{E}}} = \frac{E_{\mathrm{R}}}{1 - \frac{E_{\mathrm{R}}}{E_{\mathrm{H}}}}. \tag{78}$$

After reaching the yield stress σ_{Y}, deformation process transits to the visco-elastic–plastic range with RDA modulus expressing by Eq. (75) which can be determined using by H' expressing by Eq. (78). We are concerned here with calculations of E_{R} and H' that are systematically repeated.

5.2. Stress levels for visco-elastic–plastic yielding

The first value of RDA modulus E_R is

$$E_R^{(1)} = \frac{1}{\left(\frac{1}{E_H} + \frac{1}{E_K}\right)} = \frac{1}{\frac{1}{E_H} + \frac{\varphi^*}{E_H}} = \frac{E_H}{1+\varphi^*}. \tag{79}$$

The first modulus ratio is

$$\varphi_Y^{(1)} = \frac{E_H}{E_R^{(1)}} = \frac{\varepsilon_Y^{(1)}}{\varepsilon_P} = 1 + \varphi^*, \tag{80}$$

where $\varepsilon_Y^{(1)}$ is the first total strain

$$\varepsilon_Y^{(1)} = (1+\varphi^*)\varepsilon_P. \tag{81}$$

$\varepsilon_P = \sigma_P/E_H$ is the proportional strain. The value of yield stress σ_Y my be obtained also by using the RDA

$$\sigma_Y = \sigma_Y^{RDA} = \frac{E_H}{\frac{l_0}{k_z}\frac{k_z^3}{I_z}\frac{1}{\gamma\varphi_Y^{(1)}}} = \sigma_E \frac{\varphi_Y^{(1)}}{\varphi^*} = \sigma_E \frac{1+\varphi^*}{\varphi^*}. \tag{82}$$

The relationship $\varphi^*(\mu)$ (see Eq. (83)) which has already been formulated by Milašinović (2003), now gives a new dependence of yield stress on the Poisson's ratio (see Fig. 7).

$$\varphi^* = \frac{\left[\left(\frac{1}{1-0.001\cdot\mu}\right)^4 - 1\right]\frac{1}{2\cdot 0.001}}{1 - \left[\left(\frac{1}{1-0.001\cdot\mu}\right)^4 - 1\right]\frac{1}{2\cdot 0.001}}. \tag{83}$$

The magnitude of the yield stress depend upon the magnitudes of elasticity stress and of Poisson's ratio. The assumption of incompressibility ($\mu = 0.5$) means that σ_Y and σ_E are equal.

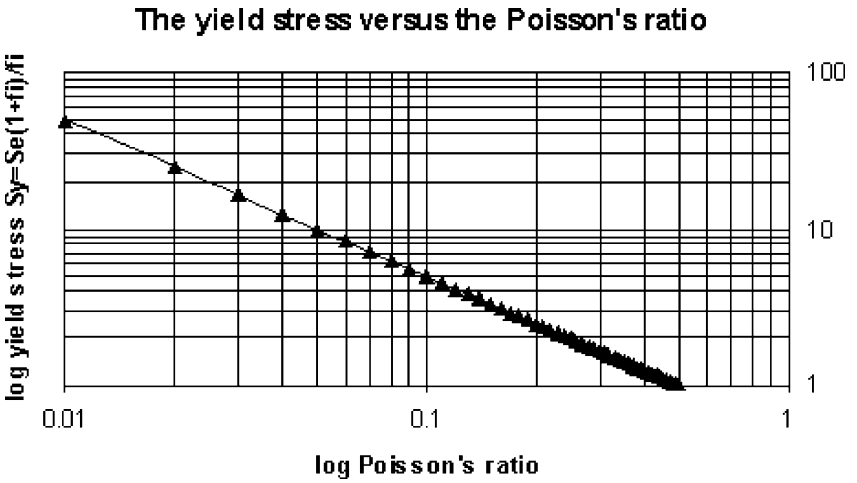

Fig. 7. Dependence of yield stress on the Poisson's ratio.

The appropriate (first) slope of the plastic strain is

$$H'^{(1)} = \frac{E_{\mathrm{R}}^{(1)}}{1 - \frac{E_{\mathrm{R}}^{(1)}}{E_{\mathrm{H}}}} = \frac{\frac{E_{\mathrm{H}}}{(1+\varphi^*)}}{1 - \frac{1}{(1+\varphi^*)}} = \frac{E_{\mathrm{H}}}{\varphi^*}. \tag{84}$$

A lower yield point can be obtained from the yield condition of the RDA, which is based on the assumption of plasticity

$$Y_{\mathrm{p}}^{(1)} = Y_{\mathrm{L}} = \sigma_{\mathrm{Y}} + H'^{(1)}\varepsilon_{\mathrm{p}}^{(1)}, \tag{85}$$

where $\varepsilon_{\mathrm{p}}^{(1)}$ is the first plastic strain

$$\varepsilon_{\mathrm{p}}^{(1)} = \frac{\varepsilon_{\mathrm{vp}}^{(1)}}{\varphi_{\mathrm{Y}}^{(1)}} = \frac{\varepsilon_{\mathrm{vp}}^{(1)}}{1+\varphi^*}. \tag{86}$$

The strain $\varepsilon_{\mathrm{vp}}^{(1)}$ the is the first visco-plastic strain, which may be obtained from the first total strain as follows:

$$\varepsilon_{\mathrm{vp}}^{(1)} = \varepsilon_{\mathrm{Y}}^{(1)} - \varepsilon_{\mathrm{E}} - \varepsilon_{\mathrm{ve}} = (1+\varphi^*)\varepsilon_{\mathrm{P}} - (1+\varphi^*)\varepsilon_{\mathrm{E}} = (1+\varphi^*)(\varepsilon_{\mathrm{P}} - \varepsilon_{\mathrm{E}}). \tag{87}$$

Consequently,

$$Y_{\mathrm{p}}^{(1)} = Y_{\mathrm{L}} = \sigma_{\mathrm{Y}} + \frac{E_{\mathrm{H}}}{\varphi^*}(\varepsilon_{\mathrm{P}} - \varepsilon_{\mathrm{E}}). \tag{88}$$

In ductile materials like metals the elastic strain ε_{E} is greater than the proportional strain ε_{P} and this is range when material instability due to the transition from an upper to a lower yield point appears.

The rate of convergence of stresses Y_{p} for this iterative procedure depends upon the physical characteristics of metals and dimensions of the bars. The procedure of determining the another stress levels for plastic yielding $1 < i > n$ continues until the magnitude of the error of the stress level becomes lesser than some previously assigned value

$$\begin{aligned}
E_{\mathrm{R}}^{(i)} &= \frac{1}{\left(\frac{1}{E_{\mathrm{H}}} + \frac{1}{E_{\mathrm{K}}} + \frac{1}{H'^{(i-1)}}\right)} = \frac{1}{\frac{1}{E_{\mathrm{H}}} + \frac{\varphi^*}{E_{\mathrm{H}}} + \frac{(i-1)\varphi^*}{E_{\mathrm{H}}}} = \frac{E_{\mathrm{H}}}{1+\mathrm{i}\varphi^*},\\
\varphi_{\mathrm{Y}}^{(i)} &= \frac{E_{\mathrm{H}}}{E_{\mathrm{R}}^{(i)}} = \frac{\varepsilon_{\mathrm{Y}}^{(i)}}{\varepsilon_{\mathrm{P}}} = 1 + \mathrm{i}\varphi^*,\\
\varepsilon_{\mathrm{Y}}^{(i)} &= (1+\mathrm{i}\varphi^*)\varepsilon_{\mathrm{P}},\\
H'^{(i)} &= \frac{E_{\mathrm{R}}^{(i)}}{1 - \frac{E_{\mathrm{R}}^{(i)}}{E_{\mathrm{H}}}} = \frac{\frac{E_{\mathrm{H}}}{(1+\mathrm{i}\varphi^*)}}{1 - \frac{1}{(1+\mathrm{i}\varphi^*)}} = \frac{E_{\mathrm{H}}}{\mathrm{i}\varphi^*},\\
\varepsilon_{\mathrm{vp}}^{(i)} &= \varepsilon_{\mathrm{Y}}^{(i)} - \varepsilon_{\mathrm{E}} - \varepsilon_{\mathrm{ve}} = (1+\mathrm{i}\varphi^*)\varepsilon_{\mathrm{P}} - (1+\varphi^*)\varepsilon_{\mathrm{E}},\\
\varepsilon_{\mathrm{p}}^{(i)} &= \frac{\varepsilon_{\mathrm{vp}}^{(i)}}{\varphi_{\mathrm{Y}}^{(i)}} = \varepsilon_{\mathrm{P}} - \frac{1+\varphi^*}{1+\mathrm{i}\varphi^*}\varepsilon_{\mathrm{E}},\\
Y_{\mathrm{p}}^{(i)} &= \sigma_{\mathrm{Y}} + H'^{(i)}\varepsilon_{\mathrm{p}}^{(i)} = \sigma_{\mathrm{Y}} + \frac{E_{\mathrm{H}}}{\mathrm{i}\varphi^*}\left(\varepsilon_{\mathrm{P}} - \frac{1+\varphi^*}{1+\mathrm{i}\varphi^*}\varepsilon_{\mathrm{E}}\right).
\end{aligned} \tag{89}$$

5.2.1. Steel bar as prototype

Structural creep coefficient of tested reinforced steel bar has already been formulated by Milašinović (2003) as follows:

$$\varphi^* = \frac{\left[\left(\frac{1}{1-0.001\cdot 0.333}\right)^4 - 1\right]\frac{1}{2\cdot 0.001}}{1 - \left[\left(\frac{1}{1-0.001\cdot 0.333}\right)^4 - 1\right]\frac{1}{2\cdot 0.001}} = 2,$$

where $\mu = 0.333$ is Poisson's ratio. On the other hand if we use Eq. (73), we have the same value

$$\varphi^* = \frac{\pi}{4 l_0 \gamma} = \frac{\pi}{4 \cdot 50 \cdot 7.86 \times 10^{-3}} = 2.$$

Using the procedure outlined in Section 5.2, the yield stress σ_Y and a lower yield stress Y_L may be calculated from the first iteration

$$E_R^{(1)} = \frac{E_H}{1+\varphi^*} = \frac{E_H}{3},$$

$$\varphi_Y^{(1)} = 1 + \varphi^* = 3,$$

$$\varepsilon_Y^{(1)} = (1+\varphi^*)\cdot \varepsilon_P = 3 \cdot 0.000677 = 0.002029,$$

$$\sigma_Y^{RDA} = \frac{E_H}{\frac{l_0}{k_z}\cdot\frac{k_z^3}{I_z}\cdot\frac{1}{\gamma\cdot\varphi_Y^{(1)}}} = \frac{210\,000 \cdot 7.86 \times 10^{-3} \cdot 3}{105.26 \cdot 0.1675315} = 280.66 \text{ MPa},$$

$$\varepsilon_{vp}^{(1)} = (1+\varphi^*)\cdot(\varepsilon_P - \varepsilon_E) = 3\cdot(\varepsilon_P - \varepsilon_E),$$

$$\varepsilon_p^{(1)} = \frac{\varepsilon_{vp}^{(1)}}{1+\varphi^*} = \varepsilon_P - \varepsilon_E = 0.000677 - 0.000891,$$

$$H'^{(1)} = \frac{E_H}{\varphi^*} = \frac{E_H}{2},$$

$$Y_L = \sigma_Y + H'^{(1)}\cdot\varepsilon_p^{(1)} = 280.66 + \frac{210\,000}{2}\cdot(0.000677 - 0.000891) = 258.17 \text{ MPa}.$$

The results of the next iterations are presented in Table 4. The low-carbon steel Fe E275 and order metals from Table 4 belong to the group of ductile materials. After the considerable residual strains the convergences of stress levels are finished, as shown in Fig. 8.

5.2.2. Metallic bars as true models

Assuming the RDA similitude of metallic bars (see Section 4.4) we obtain the table (Table 4) of the total strains and the stress levels for visco-elastic–plastic yielding.

The resulted of total stains and stress levels for visco-elastic–plastic yielding of metallic bars in form of isochronous stress–strain diagrams are shown in Fig. 8.

6. Visco-plastic range

6.1. Stress levels for strain hardening branch

If we wish to take into account the effect of visco-plastic strain to the stress level, two different procedures are presented in the literature. One procedure is used to approximate the behavior by mechanical

Table 4
Total strains and stress levels for visco-elastic–plastic yielding of metallic bars

	Aluminum	Copper	Brass	Lead	Steel prototype
E_H [N/m^2]	69 600 000 000	1.16E + 11	90 200 000 000	15 700 000 000	2.1E + 11
φ^*	5.907559	1.967873	2.113035	2.063863	1.998469
$\varepsilon_Y^{(1)}$	0.004819	0.002513	0.00282	0.004579	0.002029
σ_Y^{RDA}[MPa]	74.74	194.97	158.42	45.84	280.66
$Y_p^{(1)} = Y_L$	72.14	179.20	146.20	42.25	258.17
$\varepsilon_Y^{(2)}$	0.00894	0.004179	0.004735	0.007664	0.003381
$Y_p^{(2)}$	75.93	200.18	162. 60	47.06	288.13
$\varepsilon_Y^{(3)}$	0.013061	0.005845	0.006649	0.010749	0.004734
$Y_p^{(3)} = Y_U$	76.15	202.20	164.11	47.51	290.99
$\varepsilon_Y^{(4)}$	0.017183	0.007511	0.008564	0.013834	0.006086
$Y_p^{(4)}$	76.04	201.96	163.89	47.45	290.64
$\varepsilon_Y^{(5)}$	0.021304	0.009178	0.010478	0.016919	0.007439
$Y_p^{(5)}$	75.89	201.36	163.41	47.31	289.78
$\varepsilon_Y^{(6)}$	0.025425	0.010844	0.012393	0.020003	0.008791
$Y_p^{(6)}$	75.77	200.76	162.93	47.17	288.91
$\varepsilon_Y^{(7)}$	0.029546	0.01251	0.014307	0.023088	0.010143
$Y_p^{(7)}$	75.66	200.22	162.51	47.04	288.14
$\varepsilon_Y^{(8)}$	0.033668	0.014176	0.016221	0.026173	0.011496
$Y_p^{(8)}$	75.57	199.76	162.14	46.94	287.48
$\varepsilon_Y^{(9)}$	0.037789	0.015842	0.018136	0.029258	0.012848
$Y_p^{(9)}$	75.50	199.36	161.83	46.84	286.92
$\varepsilon_Y^{(10)}$	0.04191	0.017508	0.02005	0.032343	0.014201
$Y_p^{(10)}$	75.44	199.02	161.57	46.77	286.43
$\varepsilon_Y^{(11)}$	0.046031	0.019175	0.021965	0.035427	0.015553
$Y_p^{(11)}$	75.38	198.73	161.34	46.70	286.01
$\varepsilon_Y^{(12)}$	0.050153	0.020841	0.023879	0.038512	0.016905
$Y_p^{(12)}$	75.34	198.48	161.14	46.64	285.65
$\varepsilon_Y^{(13)}$	0.054274	0.022507	0.025794	0.041597	0.018258
$Y_p^{(13)}$	75.30	198.25	160.96	46.59	285.33

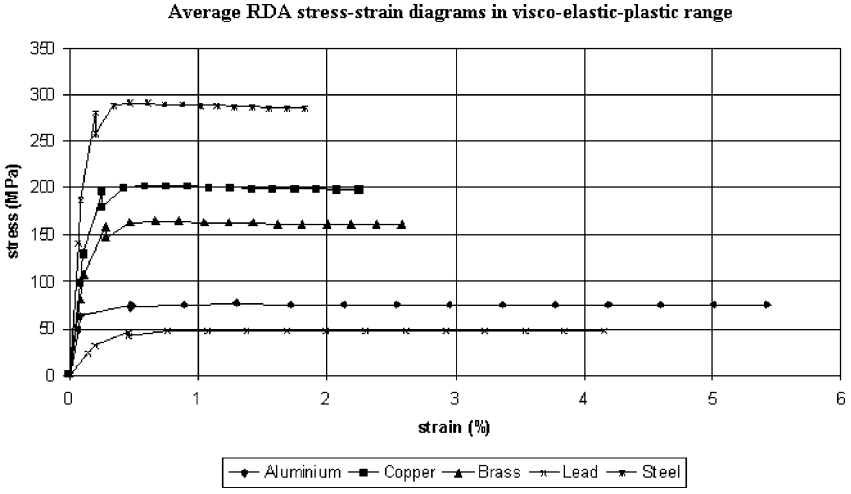

Fig. 8. Average RDA stress–strain diagrams of metallic bars in visco-elastic–plastic range according to the RDA similitude.

models. The two most widely used rules are Time Hardening Rule and the Strain Hardening Rule in which the problem is that of predicting the creep curve for stress increase.

The present paper represents an attempt to interpret the complex phenomena, with the strain hardening branch, occurring in the tensile response of metal bars through a simple previously mentioned RDA procedure. Using the procedure outlined in Section 5.2, the stress level for strain hardening branch Y_{vp} can be obtained from the yield condition as follows:

$$Y_{\mathrm{vp}} = \sigma_{\mathrm{Y}} + H'\varepsilon_{\mathrm{vp}}. \tag{90}$$

For a computed value of the first RDA modulus $E_{\mathrm{R}}^{(1)}$, the appropriate first stress level for strain hardening branch $Y_{\mathrm{vp}}^{(1)}$ may be calculated and then a new RDA modulus. The procedure of determining another stress levels for $1 < j >$m continues until the magnitude of the error of the stress level becomes lesser than some previously assigned value

$$\begin{aligned}
E_{\mathrm{R}}^{(1)} &= \frac{1}{\left(\frac{1}{E_{\mathrm{H}}}+\frac{1}{E_{\mathrm{K}}}+\frac{1}{H'}\right)} = \frac{1}{\frac{1}{E_{\mathrm{H}}}+\frac{\varphi^*}{E_{\mathrm{H}}}+\frac{\varphi^*}{E_{\mathrm{H}}}} = \frac{E_{\mathrm{H}}}{1+2\varphi^*},\\
\varphi_{\mathrm{Y}}^{(1)} &= \frac{E_{\mathrm{H}}}{E_{\mathrm{R}}^{(1)}} = 1+2\varphi^*,\\
\varepsilon_{\mathrm{Y}}^{(1)} &= \varphi_{\mathrm{Y}}^{(1)}\varepsilon_{\mathrm{P}} = (1+2\varphi^*)\varepsilon_{\mathrm{P}},\\
\varepsilon_{\mathrm{vp}}^{(1)} &= (1+2\varphi^*)\varepsilon_{\mathrm{P}} - (1+\varphi^*)\varepsilon_{\mathrm{E}},\\
H'^{(1)} &= \frac{E_{\mathrm{R}}^{(1)}}{1-\frac{E_{\mathrm{R}}^{(1)}}{E_{\mathrm{H}}}} = \frac{\frac{1}{(1+2\varphi^*)}E_{\mathrm{H}}}{1-\frac{1}{(1+2\varphi^*)}} = \frac{E_{\mathrm{H}}}{2\varphi^*},\\
Y_{\mathrm{vp}}^{(1)} &= \sigma_{\mathrm{Y}} + H'^{(1)}\varepsilon_{\mathrm{vp}}^{(1)} = \sigma_{\mathrm{Y}} + \frac{E_{\mathrm{H}}}{2\varphi^*}[(1+2\varphi^*)\varepsilon_{\mathrm{P}} - (1+\varphi^*)\varepsilon_{\mathrm{E}}].
\end{aligned} \tag{91}$$

The jth iteration

$$\begin{aligned}
E_{\mathrm{R}}^{(j)} &= \frac{1}{\left(\frac{1}{E_{\mathrm{H}}}+\frac{1}{E_{\mathrm{K}}}+\frac{1}{H'^{(j-1)}}\right)} = \frac{1}{\frac{1}{E_{\mathrm{H}}}+\frac{\varphi^*}{E_{\mathrm{H}}}+\frac{j\varphi^*}{E_{\mathrm{H}}}} = \frac{E_{\mathrm{H}}}{1+(j+1)\varphi^*},\\
\varphi_{\mathrm{Y}}^{(j)} &= \frac{E_{\mathrm{H}}}{E_{\mathrm{R}}^{(j)}} = 1+(j+1)\varphi^*,\\
\varepsilon_{\mathrm{Y}}^{(j)} &= \varphi_{\mathrm{Y}}^{(j)}\varepsilon_{\mathrm{P}} = [1+(j+1)\varphi^*]\varepsilon_{\mathrm{P}},\\
\varepsilon_{\mathrm{vp}}^{(j)} &= [1+(j+1)\varphi^*]\varepsilon_{\mathrm{P}} - (1+\varphi^*)\varepsilon_{\mathrm{E}},\\
H'^{(j)} &= \frac{E_{\mathrm{R}}^{(j)}}{1-\frac{E_{\mathrm{R}}^{(j)}}{E_{\mathrm{H}}}} = \frac{\frac{1}{1+(j+1)\varphi^*}E_{\mathrm{H}}}{1-\frac{1}{1+(j+1)\varphi^*}} = \frac{E_{\mathrm{H}}}{(j+1)\varphi^*},\\
Y_{\mathrm{vp}}^{(j)} &= \sigma_{\mathrm{Y}} + H'^{(j)}\varepsilon_{\mathrm{vp}}^{(j)} = \sigma_{\mathrm{Y}} + \frac{E_{\mathrm{H}}}{(j+1)\varphi^*}\{[1+(j+1)\varphi^*]\varepsilon_{\mathrm{P}} - (1+\varphi^*)\varepsilon_{\mathrm{E}}\}.
\end{aligned} \tag{92}$$

6.1.1. Steel bar as prototype

$$E_{\mathrm{R}}^{(1)} = \frac{E_{\mathrm{H}}}{1+2\cdot\varphi^*} = \frac{E_{\mathrm{H}}}{5},$$

$$\varphi_{\mathrm{Y}}^{(1)} = (1+2\cdot\varphi^*) = 5,$$

$$\varepsilon_{\mathrm{Y}}^{(1)} = (1+2\cdot\varphi^*)\cdot\varepsilon_{\mathrm{P}} = 5\cdot\varepsilon_{\mathrm{P}},$$

$$\varepsilon_{\mathrm{vp}}^{(1)} = (1 + 2 \cdot \varphi^*) \cdot \varepsilon_{\mathrm{P}} - (1 + \varphi^*) \cdot \varepsilon_{\mathrm{E}} = 5 \cdot 0.000677 - 3 \cdot 0.000891 = 0.000707,$$

$$H'^{(1)} = \frac{E_{\mathrm{H}}}{2 \cdot \varphi^*} = \frac{E_{\mathrm{H}}}{4},$$

$$Y_{\mathrm{vp}}^{(1)} = \sigma_{\mathrm{Y}} + H'^{(1)} \cdot \varepsilon_{\mathrm{vp}}^{(1)} = 280.66 + \frac{210000}{4} \cdot 0.000707 = 317.99 \text{ MPa}.$$

The results of the next iterations are listed in Table 5. The stress $Y_{\mathrm{vp}} = 406.64$ MPa at last iteration is in good accordance with value of fracture stress ($\sigma_C = 390$ MPa), recommended in prEN 10113: for steel Fe E275.

6.1.2. Metallic bars as true models

Assuming the RDA similitude of metallic bars we obtain the table (Table 5) of the stress levels for strain hardening branch. *After reaching ultimate residual strains the convergences of stress levels are finished, thus indicating a well-defined RDA fracture stresses as shown in Fig.* 9.

6.2. Total strain for strain hardening branch

In the initial stages of the tensile test, the cross-sectional area A of the bar almost remains constant, but beginning from the strain hardening branch stress a noticeable reduction takes place, which is initially uniform over the entire length of the specimen, and after crossing the strain hardening branch period it becomes localized. However, once the neck is formed, the relative elongation also becomes dependent upon the dimensions of the bar (its length and diameter) and thus is no more a characteristics of the material only.

As mentioned above the total strain in the visco-elasto-plastic range is

$$\varepsilon_{\mathrm{Y}}^{(i)} = \varphi_{\mathrm{Y}}^{(i)} \varepsilon_{\mathrm{P}}. \tag{93}$$

Knowing the last value $\varepsilon_{\mathrm{Y}}^{(n)}$, we can calculate the change in the value of extension of the bar under tension for strain hardening branch as

$$\varepsilon_{\mathrm{Y}}^{*(j)} = \varepsilon_{\mathrm{Y}}^{(n)} + \frac{A}{A_{\mathrm{red}}} \varepsilon_{\mathrm{Y}}^{(j)}. \tag{94}$$

A_{red} is localized reduction of cross-section area in the narrowest part of the neck.

Table 5
Stress levels for strain hardening branch of metallic bars

	Aluminum	Copper	Brass	Lead	Steel prototype
$Y_{\mathrm{up}^{(1)}}$	90.04	220.68	180.27	52.07	317.99
$Y_{\mathrm{up}^{(2)}}$	101.12	244.86	200.23	57.82	352.92
$Y_{\mathrm{up}^{(3)}}$	106.67	256.94	210.20	60.69	370.38
$Y_{\mathrm{up}^{(4)}}$	109.99	264.20	216.19	62.41	380.86
$Y_{\mathrm{up}^{(5)}}$	112.21	269.03	220.18	63.56	387.84
$Y_{\mathrm{up}^{(6)}}$	113.79	272.43	223.03	64.38	392.83
$Y_{\mathrm{up}^{(7)}}$	114.98	275.07	226.17	65.00	396.57
$Y_{\mathrm{up}^{(8)}}$	115.90	277.09	228.83	65.48	399.49
$Y_{\mathrm{up}^{(9)}}$	116.64	278.70	223.16	65.86	401.81
$Y_{\mathrm{up}^{(10)}}$	117.25	280.02	229.25	66.17	403.72
$Y_{\mathrm{up}^{(11)}}$	117.75	281.12	230.16	66.44	405.31
$Y_{\mathrm{up}^{(12)}}$	118.18	282.05	230.93	66.66	406.65

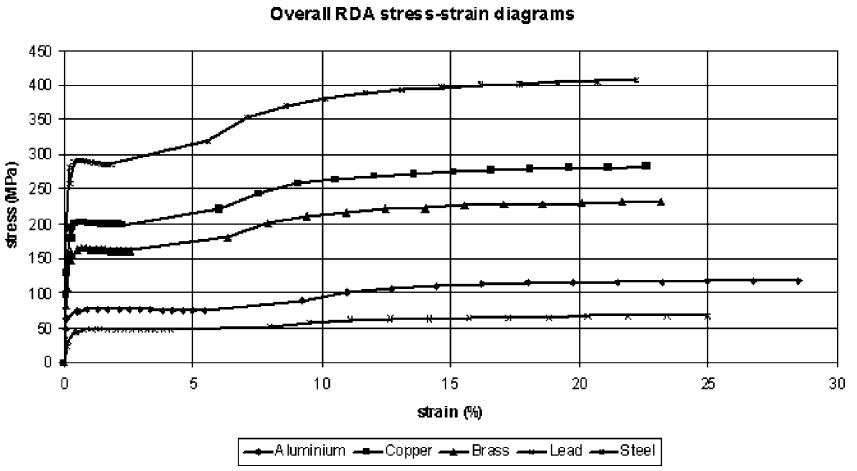

Fig. 9. Overall stress–strain diagrams for metallic bars according to the RDA similitude.

Previously, the author (Milašinović, 2003) has underscored the need to introduce a distinction between an 'original' and a 'localized reduction' cross-section area, considering the fatigue problem of metallic thin long symmetrical bars. The cross-section area in the narrowest part of the neck may be obtained by applying Bernoulli's energy theorem, taking into account the minimum strain rate creep σ_P/λ_K of material

$$\sigma_1 + \frac{1}{2}\rho A^* l_0 \dot{\varepsilon}_1^2 \frac{1}{l_0} = \sigma_2 + \frac{1}{2}\rho A^* l_0 \dot{\varepsilon}_2^2 \frac{1}{l_0} = \sigma_2 + \frac{1}{2}\rho A^* \left(\frac{A}{A_{\text{red}}}\right)^2 \dot{\varepsilon}_1^2, \tag{95}$$

where $\sigma_1 = \sigma_P$ is applied proportional stress, $\dot{\varepsilon}_1 = \frac{\sigma_1}{\sqrt{E_H \rho}} \frac{\varphi^*}{l_0}$ is initial strain rate, $A^* = 1$ is a unit cross-sectional area and $\sigma_2 = \sigma_P/(1+\varphi^*)$ is the RDA fatigue limit in symmetrical cycle. Thus

$$\frac{A}{A_{\text{red}}} = \sqrt{\frac{2E_H l_0^2}{\sigma_P \varphi^*} \frac{1}{1+\varphi^*} + 1}. \tag{96}$$

6.2.1. Steel bar as prototype

Proportional stress as reaction-stress of clamped steel bar is $\sigma_P = 142$ MPa (see Section 3.2). Thus

$$\frac{A}{A_{\text{red}}} = \sqrt{\frac{2 \cdot 2.1 \times 10^5 \cdot 0.5^2}{142 \cdot 2} \cdot \frac{1}{1+2} + 1} = 11.15$$

and

$$\varepsilon_Y^{*(j)} = \varepsilon_Y^{(12)} + \frac{A}{A_{\text{red}}} \cdot \varepsilon_Y^{(i)} = \varepsilon_Y^{(12)} + 11.15 \cdot \varepsilon_Y^{(j)}.$$

We then obtain

$$\varepsilon_Y^{(1)} = (1 + 2 \cdot \varphi^*) = 5 \cdot \varepsilon_P,$$

$$\varepsilon_Y^{*(1)} = 0.018258 + 11.15 \cdot 5 \cdot 0.000677 = 0.056001.$$

Table 6
Total strains for strain hardening branch of metallic bars

	Aluminum	Copper	Brass	Lead	Steel prototype
E_H [N/m^2]	69 600 000 000	1.16E + 11	90 200 000 000	157 000 000 000	2.1E + 11
φ^*	5.907559	1.967573	2.113035	2.063863	1.998469
l_0 [cm]	49.24	44.70	43.22	33.647	50
σ_p [MPa]	48.554622	98.23	81.72228	23.466327	142.00
A/A_{red}	4.246626	9.04552	79.80394	4.995701	11.15333
$\varepsilon_Y^{*(1)}$ [%]	9.2239	6.0309	6.358	79 885	5.5973
$\varepsilon_Y^{*(2)}$	10.9741	7.5381	7.8858	9.5296	7.1056
$\varepsilon_Y^{*(3)}$	12.72423	9.045202	9.413611	11.07068	8.613975
$\varepsilon_Y^{*(4)}$	14.4744	10.5523	10.9414	12.6118	10.1223
$\varepsilon_Y^{*(5)}$	16.2245	12.0595	12.4692	14.1528	11.6307
$\varepsilon_Y^{*(6)}$	17.9747	13.5666	13.997	15.6939	13.139
$\varepsilon_Y^{*(7)}$	19.7248	15.07372	15.53479	17.23497	14.6474
$\varepsilon_Y^{*(8)}$	21.4749	16.5809	17.0526	18.776	16.1558
$\varepsilon_Y^{*(9)}$	23.2251	18.088	18.5804	20.3171	17.6641
$\varepsilon_Y^{*(10)}$	24.97522	19.59511	20.10317	21.85818	19.17246
$\varepsilon_Y^{*(11)}$	26.7254	21.1022	21.636	23.3993	20.6803
$\varepsilon_Y^{*(12)}$	28.4755	22.6094	23.1638	24.9403	22.1892

The results of the next iterations are listed in Table 6.

6.2.2. Metallic bars as true models

Assuming the RDA similitude of metallic bars we obtain the table (Table 6) of the total strains for strain hardening branch.

After secondary creep range the material again starts resisting further tensile strain and to elongate it by a length Δl the force should be increased.

7. Numerical test

The computational efficiency of the algorithm described in the previous sections was verified to the example, the results of which are known in literature (Froli and Royer-Carfagni, 2000). In the order to simulate experimental results, they refer to the test reported in their paper, where the specimen presented approximately

- Diameter of the bar $\phi = 1.6$ cm
- Young's modulus $E_H = 2 \times 10^5$ MPa
- Upper yield stress $Y_U = 390$ MPa
- Lower yield point $Y_L = 358$ MPa

The yield stress $Y_L = 358$ MPa is in good accordance with yield value of mild-steel Fe E355 recommended in prEN 10113: ($\sigma_Y = 355$ N/mm^2).

7.1. RDA results

7.1.1. Proportional stress

The values of physical parameters of mild-steel: c, α_T, ρ and E_H are taken from the handbook of Modern Physics (Williams et al., 1968); specific heat [kcal/kg °C]: 0.1395; density [kg/m^3]: 7850; coefficient of linear expansion [1/°C]: 0.0000105; elastic modulus [N/m^2]: 2×10^{11}

$$\sigma_{\mathrm{P}} = \frac{2 \cdot \rho \cdot c}{\alpha_{\mathrm{T}}} = \frac{2 \cdot 7850 \cdot 0.1395}{0.0000105} = 2.0859 \times 10^{8}\ \mathrm{N/m^2} = 208.59\ \mathrm{MPa},$$

$$\varepsilon_{\mathrm{P}} = \frac{\sigma_{\mathrm{P}}}{E_{\mathrm{H}}} = \frac{208.59 \times 10^{6}}{2 \times 10^{11}} = 0.001043.$$

7.1.2. Elasticity stress

Assuming the RDA similitude of metallic bars (prototype: $l_0 = 50$ cm, $A = 1.9^2 \times \pi/4 = 2.835$ cm^2, $\varepsilon_{\mathrm{P}} = 0.000677$; true model: $A = 1.6^2 \times \pi/4 = 2.01$ cm^2, $\varepsilon_{\mathrm{P}} = 0.001043$) we may determine the elasticity stress taking into account the RDA Euler number.

$$l_{0,\mathrm{tm}} = l_{0,\mathrm{pr}} \cdot \sqrt{\frac{A_{\mathrm{tm}}}{A_{\mathrm{pr}}} \cdot \frac{\varepsilon_{P,\mathrm{pr}}}{\varepsilon_{P,\mathrm{tm}}}} = 50 \cdot \sqrt{\frac{2.01}{2.835} \cdot \frac{0.000677}{0.001043}} = 33.92\ \mathrm{cm},$$

$$k_z = \sqrt{\frac{I_z}{A}} = \frac{\phi}{4} = \frac{1.6}{4} = 0.4\ \mathrm{cm}, \quad \left(\frac{l_0}{k_z}\right)_{\mathrm{E}} = \frac{33.92}{0.4} = 84.8, \frac{k_z^3}{I_z} = \frac{1}{\phi \cdot \pi} = \frac{1}{1.6 \cdot \pi} = 0.19894.1/\mathrm{cm}.$$

Is the fact that point of elasticity, E of steel is in good accordance with slenderness ratio of 84.8, because elastic Euler's theory for this type of low-carbon steel (Fe E355 recommended in prEN 10113:) is not valid for slenderness ratio under the 85.

$$\sigma_{\mathrm{E}} = \frac{E_{\mathrm{H}} \cdot \pi^2}{\left(\frac{l_0}{k_z}\right)_{\mathrm{E}}^2} = \frac{2 \times 10^5 \cdot \pi^2}{84.8^2} = 274.5\ \mathrm{MPa},$$

$$\varepsilon_{\mathrm{E}} = \frac{\sigma_{\mathrm{E}}}{E_{\mathrm{H}}} = \frac{274.5 \times 10^{6}}{2 \times 10^{11}} = 0.001372.$$

7.1.3. Structural (visco-elastic) creep coefficient

$$\varphi^* = \frac{\pi}{4 \cdot l_0 \cdot \gamma} = \frac{\pi}{4 \cdot 33.92 \cdot 7.85 \times 10^{-3}} = 2.95$$

7.1.4. Stress levels for plastic yielding

The first iteration (yield stress and lower yield point)

$$E_{\mathrm{R}}^{(1)} = \frac{E_{\mathrm{H}}}{1 + \varphi^*} = \frac{E_{\mathrm{H}}}{3.95},$$

$$\varphi_{\mathrm{Y}}^{(1)} = 1 + \varphi^* = 3.95,$$

$$\varepsilon_{\mathrm{Y}}^{(1)} = (1 + \varphi^*) \cdot \varepsilon_{\mathrm{P}} = 3.95 \cdot 0.001043 = 0.00412,$$

$$\sigma_{\mathrm{Y}}^{\mathrm{RDA}} = \frac{E_{\mathrm{H}}}{\frac{l_0}{k_z} \cdot \frac{k_z^3}{I_z} \cdot \frac{1}{\gamma \cdot \varphi_{\mathrm{Y}}^{(1)}}} = \frac{200\,000 \cdot 7.85 \times 10^{-3} \cdot 3.95}{84.8 \cdot 0.19894} = 367.57\ \mathrm{MPa},$$

$$\varepsilon_{\mathrm{vp}}^{(1)} = (1 + \varphi^*) \cdot (\varepsilon_{\mathrm{P}} - \varepsilon_{\mathrm{E}}) = 3.95 \cdot (\varepsilon_{\mathrm{P}} - \varepsilon_{\mathrm{E}}),$$

$$\varepsilon_{\mathrm{p}}^{(1)} = \varepsilon_{\mathrm{P}} - \varepsilon_{\mathrm{E}} = 0.001043 - 0.001372,$$

$$H'^{(1)} = \frac{E_{\mathrm{H}}}{\varphi^*} = \frac{E_{\mathrm{H}}}{2.95},$$

$$Y_{\mathrm{L}}^{(1)} = \sigma_{\mathrm{Y}} + H'^{(1)} \cdot \varepsilon_{\mathrm{p}}^{(1)} = 367.57 + \frac{200\,000}{2.95} \cdot (0.001043 - 0.001372) = 345.23 \text{ MPa}.$$

Second iteration

$$E_{\mathrm{R}}^{(2)} = \frac{E_{\mathrm{H}}}{1 + 2 \cdot \varphi^*} = \frac{E_{\mathrm{H}}}{6.9},$$

$$\varphi_{\mathrm{Y}}^{(2)} = 1 + 2 \cdot \varphi^* = 6.9,$$

$$\varepsilon_{\mathrm{Y}}^{(2)} = (1 + 2 \cdot \varphi^*) \cdot \varepsilon_{\mathrm{P}} = 6.9 \cdot 0.001043 = 0.0072,$$

$$\varepsilon_{\mathrm{vp}}^{(2)} = (1 + 2 \cdot \varphi^*) \cdot \varepsilon_{\mathrm{P}} - (1 + \varphi^*) \cdot \varepsilon_{\mathrm{E}} = 6.9 \cdot \varepsilon_{\mathrm{P}} - 3.95 \cdot \varepsilon_{\mathrm{E}},$$

$$\varepsilon_{\mathrm{p}}^{(2)} = \varepsilon_{\mathrm{P}} - \frac{1 + \varphi^*}{1 + 2 \cdot \varphi^*} \cdot \varepsilon_{\mathrm{E}} = 0.001043 - \frac{3.95}{6.9} \cdot 0.001372,$$

$$H'^{(2)} = \frac{E_{\mathrm{H}}}{2 \cdot \varphi^*} = \frac{E_{\mathrm{H}}}{5.9},$$

$$Y_{\mathrm{p}}^{(2)} = \sigma_{\mathrm{Y}} + H'^{(2)} \cdot \varepsilon_{\mathrm{p}}^{(2)} = 367.57 + \frac{200\,000}{5.9} \cdot \left(0.001043 - \frac{3.95}{6.9} \cdot 0.001372\right) = 376.29 \text{ MPa}.$$

The third iteration (upper yield point)

$$E_{\mathrm{R}}^{(3)} = \frac{E_{\mathrm{H}}}{1 + 3 \cdot \varphi^*} = \frac{E_{\mathrm{H}}}{9.85},$$

$$\varphi_{\mathrm{Y}}^{(3)} = 1 + 3 \cdot \varphi^* = 9.85,$$

$$\varepsilon_{\mathrm{Y}}^{(3)} = (1 + 3 \cdot \varphi^*) \cdot \varepsilon_{\mathrm{P}} = 9.85 \cdot 0.001043 = 0.01027,$$

$$\varepsilon_{\mathrm{vp}}^{(3)} = (1 + 3 \cdot \varphi^*) \cdot \varepsilon_{\mathrm{P}} - (1 + \varphi^*) \cdot \varepsilon_{\mathrm{E}} = 9.85 \cdot \varepsilon_{\mathrm{P}} - 3.95 \cdot \varepsilon_{\mathrm{E}},$$

$$\varepsilon_{\mathrm{p}}^{(3)} = \varepsilon_{\mathrm{P}} - \frac{1 + \varphi^*}{1 + 3 \cdot \varphi^*} \cdot \varepsilon_{\mathrm{E}} = 0.001043 - \frac{3.95}{9.85} \cdot 0.001372,$$

$$H'^{(3)} = \frac{E_{\mathrm{H}}}{3 \cdot \varphi^*} = \frac{E_{\mathrm{H}}}{8.85},$$

$$Y_{\mathrm{U}}^{(3)} = \sigma_{\mathrm{Y}} + H'^{(3)} \cdot \varepsilon_{\mathrm{p}}^{(3)} = 367.57 + \frac{200\,000}{8.85} \cdot \left(0.001043 - \frac{3.95}{9.85} \cdot 0.001372\right) = 378.71 \text{ MPa},$$

$$\vdots$$

$$E_{\mathrm{R}}^{(13)} = \frac{E_{\mathrm{H}}}{1 + 13 \cdot \varphi^*} = \frac{E_{\mathrm{H}}}{39.35},$$

$$\varphi_{\mathrm{Y}}^{(13)} = 1 + 13 \cdot \varphi^* = 39.35,$$

$$\varepsilon_{\mathrm{Y}}^{(13)} = (1 + 13 \cdot \varphi^*) \cdot \varepsilon_{\mathrm{P}} = 39.35 \cdot 0.001043 = 0.04104,$$
$$\varepsilon_{\mathrm{vp}}^{(13)} = (1 + 13 \cdot \varphi^*) \cdot \varepsilon_{\mathrm{P}} - (1 + \varphi^*) \cdot \varepsilon_{\mathrm{E}} = 39.35 \cdot \varepsilon_{\mathrm{P}} - 3.95 \cdot \varepsilon_{\mathrm{E}},$$
$$\varepsilon_{\mathrm{p}}^{(13)} = \varepsilon_{\mathrm{P}} - \frac{1 + \varphi^*}{1 + 13 \cdot \varphi^*} \cdot \varepsilon_{\mathrm{E}} = 0.001043 - \frac{3.95}{39.35} \cdot 0.001372,$$
$$H'^{(13)} = \frac{E_{\mathrm{H}}}{13 \cdot \varphi^*} = \frac{E_{\mathrm{H}}}{38.35},$$
$$Y^{(13)} = \sigma_{\mathrm{Y}} + H'^{(13)} \cdot \varepsilon_{\mathrm{p}}^{(13)} = 367.57 + \frac{200\,000}{38.35} \cdot \left(0.001043 - \frac{3.95}{39.35} \cdot 0.001372\right) = 372.3 \text{ MPa}.$$

It will be noted from the curve in Fig. 10 that the proposed RDA provides the isochronous stress–strain diagram for visco-elastic–plastic yielding of steel bar tested by Froli and Royer-Carfagni (2000) which is similar to the mild-steel Fe E355 recommended in prEN 10113: ($\sigma_{\mathrm{Y}} = 355$ N/mm^2).

7.2. Comparison between RDA model and uniform chain-bar model

An assemblage of 50 long and 53 short elementary units, in which the short units have approximately the same length as the strain gauges used in Froli and Royer-Carfagni (1999) has been calibrated by applying their model.

The response of the composite system when its extremities (as in the experiment) are displaced apart at a velocity of $\mathrm{d}\Delta l/\mathrm{d}t = 2$ mm/min was analyzed using an Ansys finite element code. Fig. 11 shows the mean reaction-stress of the clamped edge as a function of the average strain $\Delta l/l_0$.

8. RDA loading functions for Hencky's total-strain theory

8.1. Octahedral shearing stress–octahedral shearing strain loading function

The material properties generally used in the inelastic analysis of load-carrying members are obtained from tension and compression specimens in whom the state of stress is uniaxial. If the state of stress in the load-carrying member is also uniaxial, the relation between stress and strain at any point in the member is

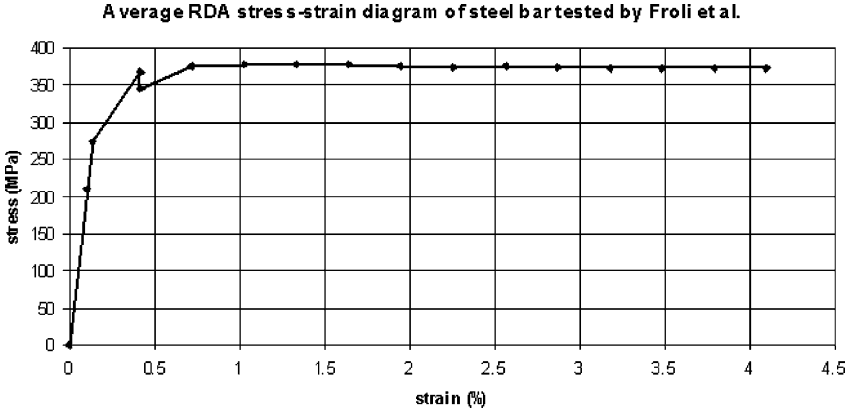

Fig. 10. Average isochronous RDA stress–strain diagram of steel bar tested by Froli and Royer-Carfagni (2000).

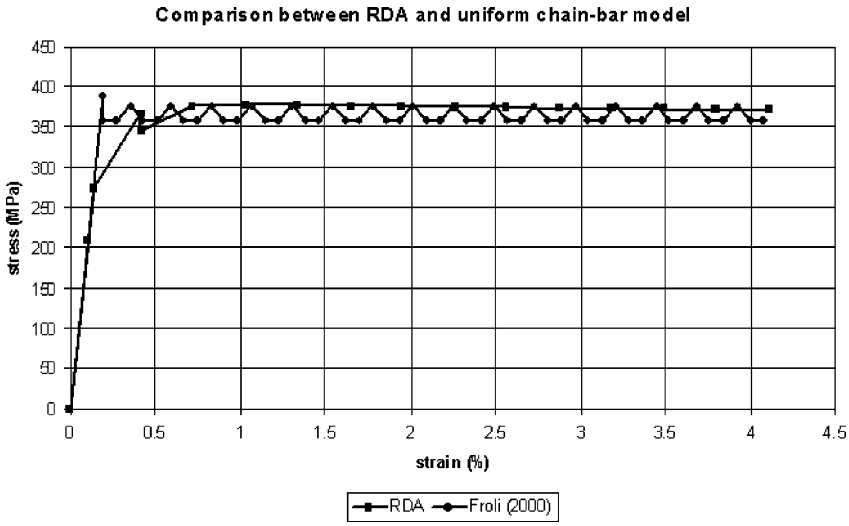

Fig. 11. Comparison between RDA model and uniform chain-bar model (Froli and Royer-Carfagni, 2000) solutions.

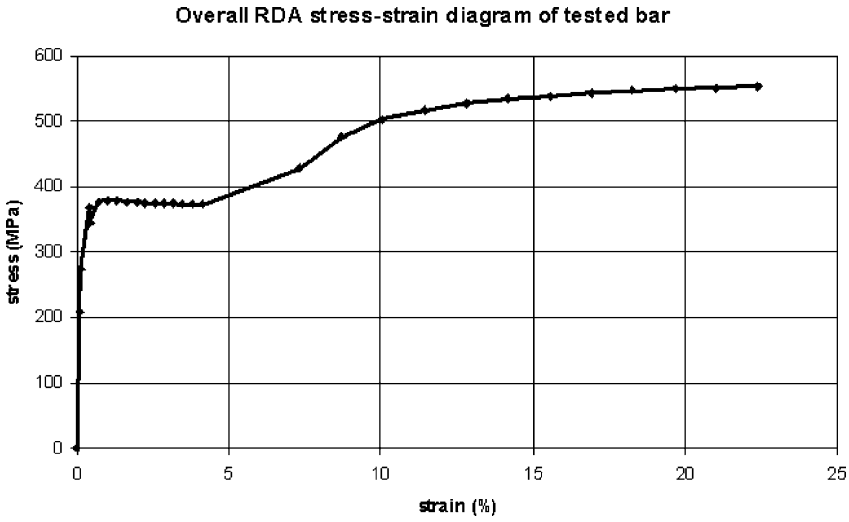

Fig. 12. Overall isochronous RDA stress–strain diagram of steel bar tested by Froli and Royer-Carfagni (2000).

identical with that obtained from tension and compression tests. If the state of stress in the load-carrying member is biaxial or triaxial, no simple stress–strain relation exists: a special function, called a yield condition is required in order to predict the beginning of inelastic strain and so that the elastic–plastic boundary in the member can be determined after inelastic strains begin. The stress–strain relation in the inelastic portion is specified by a loading function, which is based on the average of the tension and compression stress–strain diagrams. Since the loading function must be valid for all states of stress, it is convenient to first picture the loading function for simple tension.

The Hencky stress–strain relations introduce the unknown ω so that a new independent equation must be obtained from the loading function. If the von Mises yield condition is being used, the unknown ω can be obtained from as follows

$$\omega = \frac{G_{\mathrm{H}}\gamma_{\mathrm{oct}}}{\tau_{\mathrm{oct}}}. \tag{97}$$

This relation states that ω is known if corresponding values of τ_{oct} and γ_{oct} are known for any specified deformation. Thus, an octahedral shearing stress–octahedral shearing strain diagram gives the loading function. This stress–strain diagram is called the Schmidt (1932) curve by Sokolovsky (1946). In the elastic range, $\omega = 1$ so that the loading function becomes

$$\tau_{\mathrm{oct}} = G_{\mathrm{H}}\gamma_{\mathrm{oct}}. \tag{98}$$

In the inelastic range, the relation may represent the loading function

$$\tau_{\mathrm{oct}} = F(\gamma_{\mathrm{oct}}), \tag{99}$$

where the function, F, is obtained from simple tension test. Let us consider the compressible case in which μ is different from 0.5. In this case the analysis must make use of the deviatory components of stress and strain.

In the case of the tension test, let $\sigma_1 = \sigma$ so that $\sigma_2 = \sigma_3 = 0$. Thus

$$\frac{e_1}{S_1} = \frac{e_2}{S_2}, \tag{100}$$

in which

$$\begin{aligned} e_1 &= \varepsilon_1 - e = \varepsilon_1 - \frac{1}{3}(\varepsilon_1 + \varepsilon_2 + \varepsilon_3), \\ e_2 &= \varepsilon_2 - e = \varepsilon_2 - \frac{1}{3}(\varepsilon_1 + \varepsilon_2 + \varepsilon_3), \end{aligned} \tag{101}$$

$$\begin{aligned} S_1 &= \sigma_1 - S = \sigma_1 - \frac{1}{3}(\sigma_1 + \sigma_2 + \sigma_3) = \sigma_1 - \frac{1}{3}\sigma_1 = \frac{2}{3}\sigma_1 = \frac{2}{3}\sigma, \\ S_2 &= \sigma_2 - S = \sigma_2 - \frac{1}{3}(\sigma_1 + \sigma_2 + \sigma_3) = -\frac{1}{3}\sigma_1 = -\frac{1}{3}\sigma. \end{aligned} \tag{102}$$

The strain measured in the direction of σ is $\varepsilon_1 = \varepsilon$, so that

$$e_2 = \frac{e_1}{S_1}S_2 = (\varepsilon_1 - e)\left(-\frac{1}{2}\right) = -\frac{\varepsilon_1}{2} + \frac{e}{2} = -\frac{\varepsilon}{2} + \frac{e}{2}. \tag{103}$$

If the material is assumed compressible, for uniaxial state of stress, $\varepsilon_2 = \varepsilon_3 = -\mu\varepsilon$. For this condition we have

$$\begin{aligned} \gamma_{\mathrm{oct}} &= \frac{2}{3}\sqrt{(\varepsilon_1 - \varepsilon_2)^2 + (\varepsilon_2 - \varepsilon_3)^2 + (\varepsilon_3 - \varepsilon_1)^2} = \frac{2}{3}\sqrt{2(\varepsilon_1 - \varepsilon_2)^2} = \frac{2\sqrt{2}}{3}(\varepsilon_1 - \varepsilon_2) \\ &= \frac{2\sqrt{2}}{3}(\varepsilon_1 - e_2 - e) = \frac{2\sqrt{2}}{3}\left(\varepsilon + \frac{\varepsilon}{2} - \frac{e}{2} - e\right) = \sqrt{2}\varepsilon - \sqrt{2}e. \end{aligned} \tag{104}$$

Using the fact that the volume changes are elastic follows:

$$e = \frac{S}{3K_{\mathrm{H}}} = \frac{1}{3}\sigma\frac{1}{3}\frac{3(1-2\mu)}{E_{\mathrm{H}}} = \frac{1}{3}\frac{(1-2\mu)}{2G_{\mathrm{H}}(1+\mu)}\sigma. \tag{105}$$

Thus

$$\gamma_{\mathrm{oct}} = \sqrt{2}\varepsilon - \frac{\sqrt{2}}{3}\frac{(1-2\mu)}{2G_{\mathrm{H}}(1+\mu)}\sigma. \tag{106}$$

Eq. (106) can also be written in terms of τ_{oct} instead of σ

$$\gamma_{\mathrm{oct}} = \sqrt{2}\varepsilon - \frac{(1-2\mu)}{2G_{\mathrm{H}}(1+\mu)}\tau_{\mathrm{oct}}, \tag{107}$$

where

$$\tau_{\mathrm{oct}} = \frac{1}{3}\sqrt{(\sigma_1-\sigma_2)^2+(\sigma_2-\sigma_3)^2+(\sigma_3-\sigma_1)^2} = \frac{1}{3}\sqrt{2\sigma_1^2} = \frac{\sqrt{2}}{3}\sigma. \tag{108}$$

If the material is assumed incompressible, $\mu = 0.5$. For this condition Eq. (106) gives

$$\gamma_{\mathrm{oct}} = \sqrt{2}\varepsilon. \tag{109}$$

8.2. Octahedral shearing stress–octahedral shearing strain RDA diagram

In Sections 5 and 6 it was proposed that the average of the tension and compression stress–strain diagram could be approximated by $1 < i < n$ and $1 < j < m$ points in which stress and strain are closely determined by RDA. In the visco-elastic–plastic range of the RDA stress–strain diagram, $\varepsilon = \varepsilon_{\mathrm{Y}}^{(i)} = (1 + \mathrm{i}\varphi^*)\varepsilon_{\mathrm{P}}$ (see Eq. (89)). This value of ε can be substituted into Eq. (107) to give loading function $F^{(i)}$. Now, let us present the extension of von Mises yield function in the first and ith iteration where first total strain leads from Eq. (81)

$$\varepsilon_{\mathrm{Y}}^{(1)} = \varphi_{\mathrm{Y}}^{(1)}\varepsilon_{\mathrm{P}} = (1+\varphi^*)\varepsilon_{\mathrm{P}},$$

so that

$$\begin{aligned}\gamma_{\mathrm{oct},Y} &= \sqrt{2}(1+\varphi^*)\varepsilon_{\mathrm{P}} - \frac{(1-2\mu_{\mathrm{Y}}^{(1)})}{2G_{\mathrm{H}}^{(1)}(1+\mu_{\mathrm{Y}}^{(1)})}\tau_{\mathrm{oct},Y} = \sqrt{2}(1+\varphi^*)\frac{\sigma_{\mathrm{P}}}{E_{\mathrm{H}}} - \frac{(1-2\mu_{\mathrm{Y}}^{(1)})}{2G_{\mathrm{H}}^{(1)}(1+\mu_{\mathrm{Y}}^{(1)})}\tau_{\mathrm{oct},Y} \\ &= \sqrt{2}\cdot(1+\varphi^*)\frac{3}{\sqrt{2}}\tau_{\mathrm{oct},P}\frac{1}{E_{\mathrm{H}}} - \frac{(1-2\mu_{\mathrm{Y}}^{(1)})}{E_{\mathrm{H}}}\tau_{\mathrm{oct},Y} = \tau_{\mathrm{oct},Y}\left[3(1+\varphi^*)n_{\mathrm{Y}} - 1 + 2\mu_{\mathrm{Y}}^{(1)}\right]\frac{1}{E_{\mathrm{H}}},\end{aligned} \tag{110}$$

where

$$n_{\mathrm{Y}} = \frac{\tau_{\mathrm{oct},P}}{\tau_{\mathrm{oct},Y}} = \frac{\sigma_{\mathrm{P}}}{\sigma_{\mathrm{Y}}}. \tag{111}$$

The inverse relationship of $\varphi^*(\mu)$ (see Eq. (83)) is defined by

$$\mu_{\mathrm{Y}}^{(1)} = \left[1 - \frac{1}{\sqrt[4]{0.002\left(\frac{\varphi_{\mathrm{Y}}^{(1)}}{1+\varphi_{\mathrm{Y}}^{(1)}}\right)+1}}\right]1000. \tag{112}$$

Thus

$$F_{\mathrm{Y}} = \frac{E_{\mathrm{H}}}{3(1+\varphi^*)n_{\mathrm{Y}} - 1 + 2\mu_{\mathrm{Y}}^{(1)}}. \tag{113}$$

Lower yield point $Y_{\mathrm{p}}^{(1)} = Y_{\mathrm{L}}$ (see Eq. (88)) is obtained from the yield condition, which is based on the assumption of plasticity and can be substituted into Eq. (110) to give

$$\gamma_{\mathrm{oct}}^{(1)} = \tau_{\mathrm{oct}}^{(1)}\left[3(1+\varphi^*)n_{\mathrm{Y}}^{(1)} - 1 + 2\mu_{\mathrm{Y}}^{(1)}\right]\frac{1}{E_{\mathrm{H}}}, \tag{114}$$

where

$$n_{\mathrm{Y}}^{(1)} = \frac{\tau_{\mathrm{oct},P}}{\tau_{\mathrm{oct}}^{(1)}} = \frac{\sigma_{\mathrm{P}}}{Y_{\mathrm{p}}^{(1)}} = \frac{\sigma_{\mathrm{P}}}{\sigma_{\mathrm{Y}} + \frac{E_{\mathrm{H}}}{\varphi^*}(\varepsilon_{\mathrm{P}} - \varepsilon_{\mathrm{E}})}. \tag{115}$$

Thus

$$F^{(1)} = \frac{E_{\mathrm{H}}}{3(1+\varphi^*)n_{\mathrm{Y}}^{(1)} - 1 + 2\mu_{\mathrm{Y}}^{(1)}}. \tag{116}$$

The ith total strain leads from Eqs. (89)

$$\varepsilon_{\mathrm{Y}}^{(i)} = \varphi_{\mathrm{Y}}^{(i)}\varepsilon_{\mathrm{P}} = (1+\mathrm{i}\varphi^*)\varepsilon_{\mathrm{P}}.$$

Thus

$$\gamma_{\mathrm{oct}}^{(i)} = \tau_{\mathrm{oct}}^{(i)}\left[3(1+\mathrm{i}\varphi^*)n_{\mathrm{Y}}^{(i)} - 1 + 2\mu_{\mathrm{Y}}^{(i)}\right]\frac{1}{E_{\mathrm{H}}}, \tag{117}$$

where

$$n_{\mathrm{Y}}^{(i)} = \frac{\tau_{\mathrm{oct,P}}}{\tau_{\mathrm{oct}}^{(i)}} = \frac{\sigma_{\mathrm{P}}}{Y_{\mathrm{p}}^{(i)}} = \frac{\sigma_{\mathrm{P}}}{\sigma_{\mathrm{Y}} + \frac{E_{\mathrm{H}}}{\mathrm{i}\varphi^*}\left(\varepsilon_{\mathrm{P}} - \frac{1+\varphi^*}{1+\mathrm{i}\varphi^*}\varepsilon_{\mathrm{E}}\right)} \tag{118}$$

and

$$\mu_{\mathrm{Y}}^{(i)} = \left[1 - \frac{1}{\sqrt[4]{0.002\left(\frac{\varphi_{\mathrm{Y}}^{(i)}}{1+\varphi_{\mathrm{Y}}^{(i)}}\right) + 1}}\right]1000. \tag{119}$$

Thus

$$F^{(i)} = \frac{E_{\mathrm{H}}}{3(1+\mathrm{i}\varphi^*)n_{\mathrm{Y}}^{(i)} - 1 + 2\mu_{\mathrm{Y}}^{(i)}}. \tag{120}$$

Table 7 presents determining τ_{oct} and γ_{oct} of metals in the visco-elastic–plastic range, which are analyzed in this paper. Octahedral shearing stress–octahedral shearing strain diagrams in this range are shown in Figs. 13 and 14.

In the visco-plastic range of the RDA stress–strain diagram, $\varepsilon = \varepsilon_{\mathrm{Y}}^{*(j)}$ (see Eq. (94)). It will be seen from Table 7 that for the last ($n = 13$) visco-elastic–plastic strain of all metallic bars, Poisson ration is practically equal to 0.5. Therefore the value of ε can be substituted into Eq. (109) to give loading function $F^{(j)}$.

Table 7
RDA procedure for determining octahedral shearing stress and octahedral shearing strain of metals in the visco-elastic–plastic range

	Aluminum	Copper	Brass	Lead	Steel prototype
E_H [MPa]	69 600	116 000	90 200	15 700	210 000
φ^*	5.907559	1967573	2.113035	2.063863	1.998469
μ	0.427196	0.331206	0.339042	0.336251	0.333333
G_H [MPa]	24383	43570	33681	5875	78750
$\tau_{oct,p}$	22.89	46.31	38.52	11.06	66.94
$\gamma_{oct,p}$	0.000939	0.001063	0.001144	0.001883	0.000850
$\tau_{oct,E}$	30.132	60.94	50.69	14.56	88.15
$\gamma_{oct,E}$	0.001236	0.001399	0.001505	0.002478	0.001119
$\varphi_Y^{(1)}$	6.907559	2.967573	3.113035	3.063863	2.998469
$\mu_Y^{(1)}$	0.436293	0.373629	0.378078	0.37661	0.374601
$\tau_{oct,Y}$	35.23	91.91	74.68	21.61	132.30
n_Y	0.649585	0.503821	0.515844	0.511998	0.505950
$\gamma_{oct,Y}$	0.006749	0.003354	0.003787	0.006138	0.002709
$\tau_{oct}^{(1)}$	34.00	84.48	68.92	19.92	121.70
$n_Y^{(1)}$	0.672997	0.548158	0.558960	0.555503	0.550025
$\gamma_{oct}^{(1)}$	0.006751	0.00337	0.003802	0.006165	0.002722
$\varphi_Y^{(2)}$	12.815118	4.935146	5.22607	5.127726	4.996938
$\mu_Y^{(2)}$	0.463271	0.415324	0.419253	0.417967	0.416191
$\tau_{oct}^{(2)}$	35.79	94.37	76.65	22.18	135.33
$n_Y^{(2)}$	0.639405	0.490708	0.502583	0.498725	0.492833
$\gamma_{oct}^{(2)}$	0.012603	0.005773	0.006559	0.0100607	0.00467
$\varphi_Y^{(3)}$	18.722677	6.902719	7.339105	7.191589	6.995407
$\mu_Y^{(3)}$	0.474086	0.436254	0.439558	0.438481	0.436986
$\tau_{oct}^{(3)}$	35.90	95.32	77.36	22.40	137.17
$n_Y^{(3)}$	0.637557	0.485805	0.497959	0.494001	0.487989
$\gamma_{oct}^{(3)}$	0.018444	0.008162	0.009299	0.015031	0.006607
$\varphi_Y^{(4)}$	24.630236	8.870292	9.45214	9.255452	8.993876
$\mu_Y^{(4)}$	0.479915	0.448839	0.451652	0.450737	0.449464
$\tau_{oct}^{(4)}$	35.85	95.20	77.26	22.36	137.01
$n_Y^{(4)}$	0.638480	0.486383	0.498627	0.494626	0.488577
$\gamma_{oct}^{(4)}$	0.02428	0.010538	0.012028	0.019478	0.008535
$\varphi_Y^{(5)}$	30.537795	10.837865	11.565175	11.319315	10.992345
$\mu_Y^{(5)}$	0.483561	0.45724	0.459679	0.458886	0.457782
$\tau_{oct}^{(5)}$	35.77	94.92	77.03	22.30	136.60
$n_Y^{(5)}$	0.639742	0.487833	0.500092	0.496090	0.490027
$\gamma_{oct}^{(5)}$	0.030104	0.012909	0.014749	0.023811	0.010457
$\varphi_Y^{(6)}$	36.445354	12.805438	13.67821	13.383178	12.990814
$\mu_Y^{(6)}$	0.486056	0.463245	0.465394	0.464697	0.463724
$\tau_{oct}^{(6)}$	35.72	94.64	76.81	22.24	136.19
$n_Y^{(6)}$	0.640755	0.489291	0.501565	0.497562	0.491503
$\gamma_{oct}^{(6)}$	0.035941	0.015276	0.017467	0.028198	0.012375
$\varphi_Y^{(7)}$	42.352913	14.773011	15.791245	15.447041	14.989283
$\mu_Y^{(7)}$	0.487871	0.467753	0.469671	0.469049	0.468181
$\tau_{oct}^{(7)}$	35.67	94.38	76.61	22.17	135.83
$n_Y^{(7)}$	0.641686	0.490610	0.502861	0.498937	0.492816
$\gamma_{oct}^{(7)}$	0.041773	0.017638	0.020182	0.032562	0.014293

Table 7 (*continued*)

	Aluminum	Copper	Brass	Lead	Steel prototype
$\varphi_{\mathrm{Y}}^{(8)}$	48.260472	16.740584	1790428	17.510904	16.987752
$\mu_{\mathrm{Y}}^{(8)}$	0.489251	0.47126	0.472991	0.47243	0.471647
$\tau_{\mathrm{oct}}^{(8)}$	35.62	94.17	76.43	22.13	135.52
$n_{\mathrm{Y}}^{(8)}$	0.642451	0.491740	0.504009	0.500000	0.493947
$\gamma_{\mathrm{oct}}^{(8)}$	0.047592	0.020002	0.022893	0.036946	0.016208
$\varphi_{\mathrm{Y}}^{(9)}$	54.168031	18.708157	20.017315	19.574767	18.986221
$\mu_{\mathrm{Y}}^{(9)}$	0.490335	0.474067	0.475644	0.475133	0.47442
$\tau_{\mathrm{oct}}^{(9)}$	35.59	93.98	76.29	22.08	135.26
$n_{\mathrm{Y}}^{(9)}$	0.643046	0.492727	0.504974	0.501067	0.494911
$\gamma_{\mathrm{oct}}^{(9)}$	0.053425	0.022363	0.025607	0.041312	0.018124
$\varphi_{\mathrm{Y}}^{(10)}$	60.07559	20.67573	22.13035	21.63863	2098469
$\mu_{\mathrm{Y}}^{(10)}$	0.49121	0.476365	0.477812	0.477344	0.476688
$\tau_{\mathrm{oct}}^{(10)}$	35.56	93.82	76.16	22.05	135.02
$n_{\mathrm{Y}}^{(10)}$	0.643558	0.493568	0.505787	0.501817	0.495758
$\gamma_{\mathrm{oct}}^{(10)}$	0.059251	0.024723	0.028315	0.045688	0.020037
$\varphi_{\mathrm{Y}}^{(11)}$	65.983149	22.643303	24.243385	23.702493	22.983159
$\mu_{\mathrm{Y}}^{(11)}$	0.49193	0.47828	0.479617	0.479185	0.478579
$\tau_{\mathrm{oct}}^{(11)}$	35.53	93.68	76.06	22.01	134.83
$n_{\mathrm{Y}}^{(11)}$	0.644070	0.494289	0.506508	0.502570	0.496486
$\gamma_{\mathrm{oct}}^{(11)}$	0.065076	0.027081	0.031029	0.050041	0.021951
$\varphi_{\mathrm{Y}}^{(12)}$	71.890708	24.610876	26.35642	25.766356	24.981628
$\mu_{\mathrm{Y}}^{(12)}$	0.492533	0.479901	0.481143	0.480741	0.480179
$\tau_{\mathrm{oct}}^{(12)}$	35.52	93.56	75.96	21.99	134.66
$n_{\mathrm{Y}}^{(12)}$	0.644412	0.494911	0.507137	0.503216	0.497112
$\gamma_{\mathrm{oct}}^{(12)}$	0.070921	0.029439	0.033737	0.054428	0.023865
$\varphi_{\mathrm{Y}}^{(13)}$	77.798267	26.578449	23.469455	27.830219	26.980097
$\mu_{\mathrm{Y}}^{(13)}$	0.493046	0.48129	0.482451	0.482076	0.48155
$\tau_{\mathrm{oct}}^{(13)}$	35.50	93.46	75.88	21.96	134.51
$n_{\mathrm{Y}}^{(13)}$	0.644754	0.495485	0.507704	0.503756	0.497669
$\gamma_{\mathrm{oct}}^{(13)}$	0.076747	0.031801	0.036449	0.058779	0.025778

$$\begin{aligned}\gamma_{\mathrm{oct}}^{(j)} &= \sqrt{2}\varepsilon_{\mathrm{Y}}^{*(j)} = \sqrt{2}\left(\varepsilon_{\mathrm{Y}}^{(n)} + \frac{A}{A_{\mathrm{red}}}\varepsilon_{\mathrm{Y}}^{(j)}\right) = \sqrt{2}\left\{(1+n\varphi^*) + \frac{A}{A_{\mathrm{red}}}[1+(j+1)\varphi^*]\right\}\frac{\sigma_{\mathrm{P}}}{E_{\mathrm{H}}} \\ &= 3\tau_{\mathrm{oct}}^{(j)}\left\{(1+n\varphi^*) + \frac{A}{A_{\mathrm{red}}}[1+(j+1)\varphi^*]\right\}\frac{1}{E_{\mathrm{H}}}m^{(j)} \end{aligned} \tag{121}$$

Thus

$$F^{(j)} = \frac{E_{\mathrm{H}}}{3\left\{(1+n\varphi^*) + \frac{A}{A_{\mathrm{red}}}[1+(j+1)\varphi^*]\right\}m^{(j)}}, \tag{122}$$

where

$$m^{(j)} = \frac{\tau_{\mathrm{oct},P}}{\tau_{\mathrm{oct}}^{(j)}} = \frac{\sigma_{\mathrm{P}}}{Y_{\mathrm{vp}}^{(j)}} = \frac{\sigma_{\mathrm{P}}}{\sigma_{\mathrm{Y}} + \frac{E_{\mathrm{H}}}{(j+1)\varphi^*}\{[1+(j+1)\varphi^*]\varepsilon_{\mathrm{P}} - (1+\varphi^*)\varepsilon_{\mathrm{E}}\}}. \tag{123}$$

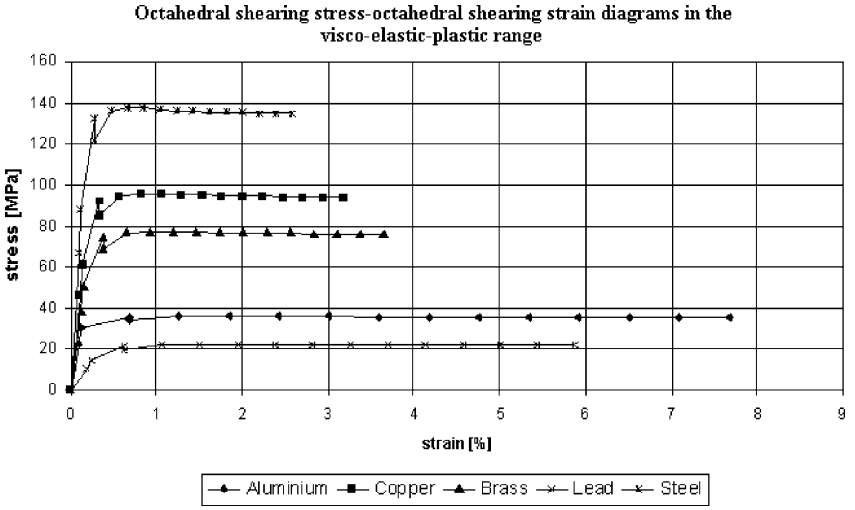

Fig. 13. Octahedral shearing stress–octahedral shearing strain diagrams of metals in the visco-elastic–plastic range.

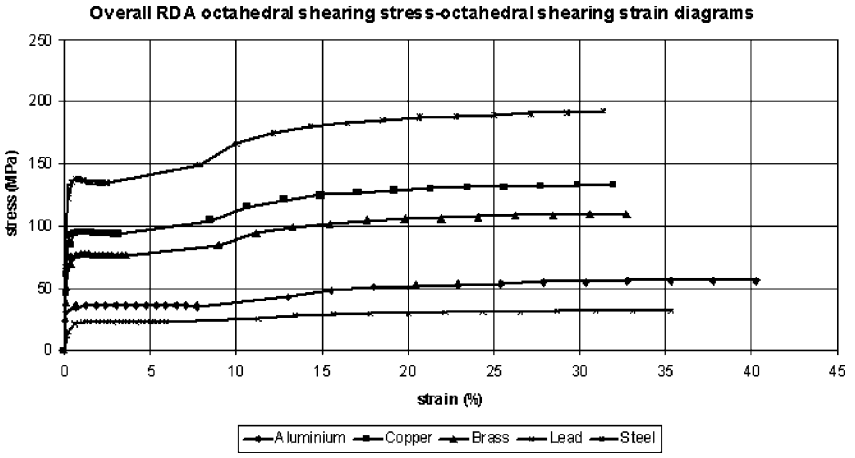

Fig. 14. Overall octahedral shearing stress–octahedral shearing strain diagrams of metals.

Table 8 presents determining τ_{oct} and γ_{oct} of metals in the visco-plastic range. These values are shown in Fig. 14.

In a hollow-torsion test, the only no vanishing components of stress and strain are $\tau_{xy} = \tau$ and $\gamma_{xy} = \gamma$. From the following equations leads:

$$\gamma_{\mathrm{oct}} = \frac{2}{3}\sqrt{(\varepsilon_x - \varepsilon_{\mathrm{Y}})^2 + (\varepsilon_{\mathrm{Y}} - \varepsilon_z)^2 + (\varepsilon_z - \varepsilon_x)^2 + \frac{3}{2}(\gamma_{xy}^2 + \gamma_{yz}^2 + \gamma_{zx}^2)} = \frac{\sqrt{2}}{\sqrt{3}}\gamma, \tag{124}$$

$$\tau_{\mathrm{oct}} = \frac{1}{3}\sqrt{(\sigma_x - \sigma_{\mathrm{Y}})^2 + (\sigma_{\mathrm{Y}} - \sigma_z)^2 + (\sigma_x - \sigma_z)^2 + 6(\tau_{xy}^2 + \tau_{yz}^2 + \tau_{xz}^2)} = \frac{\sqrt{2}}{\sqrt{3}}\tau. \tag{125}$$

This means that τ–γ diagram and the τ_{oct}–γ_{oct} diagram for a given material have similar shapes.

Table 8
RDA procedure for determining octahedral shearing stress and octahedral shearing strain of metals in the visco-plastic range

	Aluminum	Copper	Brass	Lead	Steel prototype
E_H [MPa]	69 600	116 000	90 200	15 700	210 000
φ^*	5.907559	1.967573	2.113305	2.063863	1.998469
μ	0.5	0.5	0.5	0.5	0.5
l_0 [cm]	49.24	44.70	43.22	33.647	50
σ_p [MPa]	48.55	98.23	81.72	23.47	142.00
A/A_{red}	4.246636	9.04552	7.980394	4.995701	11.15333
$m^{(1)}$	0.53920	0.44512	0.45332	0.45066	0.44655
$\gamma_{oct}^{(1)}$ [%]	13.0446	8.5290	8.9916	11.2974	7.9158
$\tau_{oct}^{(1)}$	42.45	104.03	84.98	24.55	149.90
$m^{(2)}$	0.48012	0.40117	0.40813	0.40585	0.40236
$\gamma_{oct}^{(2)}$	15.5197	10.6605	11.1522	13.4769	10.0488
$\tau_{oct}^{(2)}$	47.67	115.43	94.39	27.26	166.37
$m^{(3)}$	0.45514	0.38231	0.38877	0.38665	0.38339
$\gamma_{oct}^{(3)}$	17.9948	12.7918	13.3129	15.6563	12.1820
$\tau_{oct}^{(3)}$	50.28	121.12	99.08	28.61	174.60
$m^{(4)}$	0.44140	0.37180	0.37800	0.37600	0.37284
$\gamma_{oct}^{(4)}$	20.4699	14.9232	15.4735	17.8358	14.3151
$\tau_{oct}^{(4)}$	51.85	124.55	101.91	29.42	179.54
$m^{(5)}$	0.43267	0.36513	0.37115	0.36919	0.36613
$\gamma_{oct}^{(5)}$	22.9449	17.0547	17.6341	20.0151	16.4483
$\tau_{oct}^{(5)}$	52.90	126.82	103.79	29.96	182.83
$m^{(6)}$	0.42666	0.36050	0.36641	0.36449	0.36148
$\gamma_{oct}^{(6)}$	25.4201	19.1861	19.7947	22.1945	18.5814
$\tau_{oct}^{(6)}$	53.64	128.45	105.14	30.35	185.18
$m^{(7)}$	0.42225	0.35711	0.36293	0.36102	0.35807
$\gamma_{oct}^{(7)}$	27.8951	21.3175	21.9554	24.3739	20.7146
$\tau_{oct}^{(7)}$	54.20	129.67	106.15	30.64	186.94
$m^{(8)}$	0.41889	0.35451	0.36027	0.35837	0.35545
$\gamma_{oct}^{(8)}$	30.3701	23.4489	24.1160	26.5533	22.8478
$\tau_{oct}^{(8)}$	54.64	130.62	106.93	30.87	188.32
$m^{(9)}$	0.41624	0.35246	0.35817	0.35630	0.35340
$\gamma_{oct}^{(9)}$	32.8453	25.5803	26.2767	28.7327	24.9808
$\tau_{oct}^{(9)}$	54.98	131.38	107.56	31.05	189.42
$m^{(10)}$	0.41407	0.35080	0.35647	0.35463	0.35173
$\gamma_{oct}^{(10)}$	35.3203	27.7117	28.4372	30.9121	27.1140
$\tau_{oct}^{(10)}$	55.27	132.00	108.07	31.19	190.32
$m^{(11)}$	0.41231	0.34942	0.35505	0.35319	0.35035
$\gamma_{oct}^{(11)}$	37.7954	29.8430	30.5979	33.0916	29.2471
$\tau_{oct}^{(11)}$	55.51	132.52	108.50	31.32	191.06
$m^{(12)}$	0.41081	0.34827	0.35387	0.35203	0.34919
$\gamma_{oct}^{(12)}$	40.2704	31.9745	32.7586	35.2709	31.3803
$\tau_{oct}^{(12)}$	55.71	132.96	108.86	31.42	191.67

9. Conclusion

The RDA method has been applied to predict and described some different aspects of inelastic behavior of metallic bars.

The good agreement between RDA-predicted and measured data for the laboratory-tested steel bars gave confidence in the RDA predictions as a credible base for explanation of the phenomenon of discontinuous plastic deformation.

- Proportional stress or reaction-stress of clamped bars is obtained using physical characteristics of metal only, like as: specific heat, coefficient of linear thermal expansion and mass density.
- Elasticity stress of the bars under compression is obtained by Euler's formula and RDA similitude from which we have that elasticity stress also becomes dependent upon the dimensions of the bar (its length and diameter) and thus is no more a physical characteristics of the material only.
- In ductile materials like metals some difference between point of proportionality and point of elasticity produce the deviation from perfect elasticity with dissipation of mechanical energy through quasi-viscous flow or visco-elastic creep. This is the reason of the drop (lower-yield point) in the stress–strain curve in the average σ–ε diagrams.
- Transition from visco-elastic–plastic range beyond the lower-yield point is obtained using by iterative procedure and must be continued until the magnitude of the error of the stress level becomes lesser than some previously assigned value.
- Transition from strain hardening (visco-plastic) range with the reduction of cross-sectional area is difficult to obtain by the experimental investigations except determination the ultimate or fracture stress and strain. Above determined RDA iterative procedure through strain hardening branch (see Sections 6) may be used for comparison when alternative members under various load types are considered. After reaching ultimate residual strains the convergences of stress levels are finished, thus indicating a well-defined RDA fracture stresses as shown in Fig. 9.
- The RDA isochronous stress–strain diagram is used to predict the loading functions for the material of metallic bars. Hencky's total-strain theory is used under the assumption of compressibility in the visco-elastic–plastic and assumption of incompressibility in the strain hardening (visco-plastic) range.

References

Bell, J.F., 1973. The experimental foundations of solid mechanics. In: Handbuch der Physik, Vol. VIa/1. Springer-Verlag, Berlin.

Elam, C.F., 1938. The influence of the rate of deformation on the tensile test with special reference to the yield point in iron and steel. Proc. R. Soc., London 165, 568.

Froli, M., Royer-Carfagni, G.F., 1997. An experimental study of the Potervin–Le Chatelier effect in steel bars. In: Proceedings of the XIII National Meeting of AIMETA, Siena.

Froli, M., Royer-Carfagni, G.F., 1999. Discontinuous deformation of tensile steel bars: experimental results. ASCE, J. Eng. Mech. 125 (12), 1243–1250.

Froli, M., Royer-Carfagni, G.F., 2000. A mechanical model for the elastic–plastic behaviour of metallic bars. Int. J. Solids Struct. 37, 3901–3918.

Lempriere, B.M., 1962. Oscillations in tensile testing. Int. J. Mech. Sci. 4, 171.

Milašinović, D.D., 2000. Rheological–dynamical analogy: prediction of buckling curves of columns. Int. J. Solids Struct. 37, 3965–4004.

Milašinović, D.D., 2003. Rheological–dynamical analogy: modeling of fatigue behavior. Int. J. Solids Struct. 40, 181–217.

Miklowitz, J., 1947. The initiation and propagation of the plastic zone in a tension bar of mild steel as influenced by the speed of stretching and rigidity of testing machine. J. Appl. Mech. 14, A-31.

Polakowski, N.K., Ripling, E.J., 1966. Strength and Structure of Engineering Materials. Prentice-Hall, Inc., Englewood Cliffs, NJ.

Reiner, M., 1955. Rhéologie théorique. Dunod, Paris, France.

Schmidt, R., 1932. Ing. Arch. 3 (3), 1932.

Siebel, E., Schwaigerer, S., 1937–1938. Die Streckgrenze beim Zugversuch unter besonderer Berücksichtigung des Einflußes der Belastungsweise und der Machinenfederung. Arch. Eisenhüttenwes. 11, 319.

Sokolovsky, W.W., 1946. Theory of Plasticity. Moscow, USSR (in Russian).

Williams, J.E. et al., 1968. Modern Physics. Holt, Rinehart, and Winston, Inc., New York.